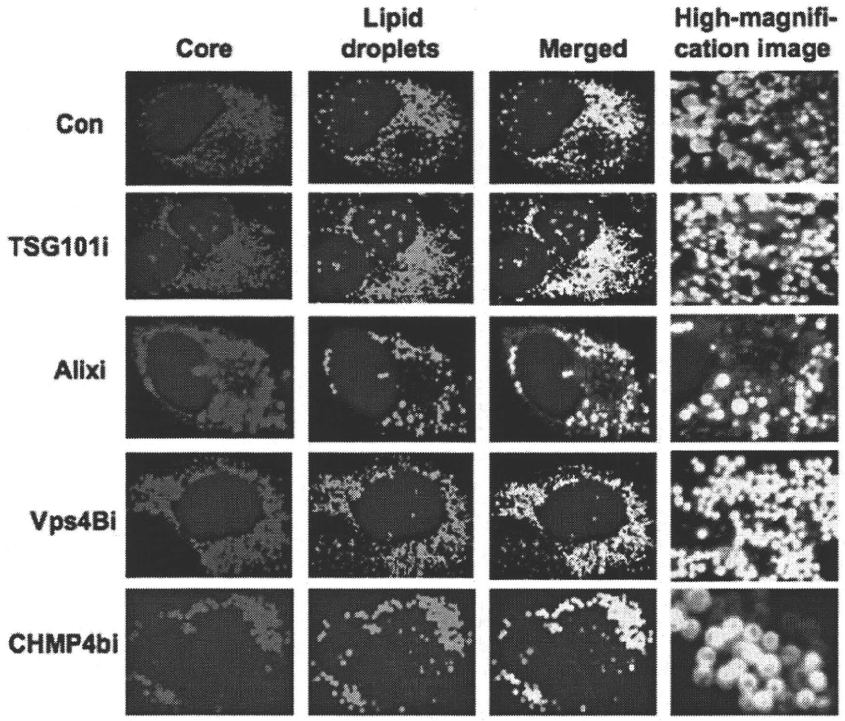

Figure 3. HCV Core is targeted to lipid droplets even in the ESCRT knockdown cells. The RSc cells transduced with a control lentiviral vector (Con), the TSG101 knockdown (TSG101i), the Alix knockdown (Alixi), the Vps4B knockdown (Vps4Bi), or the CHMP4b knockdown (CHMP4bi) cells were infected with HCV-JFH1. Cells were fixed 60 hrs post-infection and were then examined by confocal laser scanning microscopy. Cells were stained with anti-HCV Core (CP-9 and CP-11 mixture) and were then visualized with Cy3 (red). Lipid droplets and nuclei were stained with BODIPY 493/503 (green) and DAPI (blue), respectively. Images were visualized using confocal laser scanning microscopy. Colocalization is shown in yellow (Merged).
doi:10.1371/journal.pone.0014517.g003

2D), while the siRNA did not affect intracellular HCV Core level (Fig. 2E and 2F). Accordingly, we noticed some discrepancy that shRNA targeted to Vps4B or CHMP4b somewhat decreased intracellular HCV RNA replication (Fig. 1I), whereas siRNA targeted to TASG101, Alix, Vps4B or CHMP4b did not affect the RNA replication of subgenomic replicon of JFH1 (Fig. 2A and 2B). Furthermore, siRNAs targeted to TSG101, Alix, Vps4B, or CHMP4b did not affect HCV-O (genotype 1b) RNA replication using the OR6 assay system [17,18] (Fig. 2C), indicating that the ESCRT system is unrelated to the HCV RNA replication of genotype 1b. Thus, we suggested that the ESCRT system is not significant for HCV RNA replication. Within the family *Flaviviridae*, NS3 of the Japanese encephalitis virus (JEV) is also known to interact with TSG101 and microtubules, suggesting their potential roles in JEV assembly [28]. Accordingly, HCV NS3 has been involved in HCV particle assembly and infectivity [29,30]. However, whether HCV NS3 or another HCV protein binds to TSG101 remains to be investigated. At least, we did not observe the interaction between HCV NS5A and CHMP4b (Fig. 4D), Alix (Fig. 4D), TSG101, or Vps4B (data not shown).

Efficient enveloped virus release requires *cis*-acting viral late domains (L-domains), including P(T/S)AP, YPXnL (where X is any amino acid), and PPXY amino acid L-domain motif that are found in the structural proteins of other enveloped viruses [10,11]. Unlike the case with these enveloped viruses, we failed to find the three types of conserved viral L-domain motif in the HCV-JFH1 Core (data not shown). Nevertheless, we observed that the Core bound to CHMP4b, whereas NS5A did not (Fig. 4D), suggesting that the Core has a novel motif required for the HCV production. In this regard, Blanchard *et al.* reported that the aspartic acid at position 111 in the Core is crucial for virus assembly [31]. Interestingly, the conversion of the aspartic acid into alanine at amino acid 111 (PTDP to PTAP), which creates the PTAP L-domain motif, enhanced the release of HCV Core in the cell culture medium (a 2.5-fold increase) compared with the wild-type Core [31]. In contrast, Klein *et al.* demonstrated that the D111A mutation in the Core had no effect on HCV capsid assembly [32]. Furthermore, Murray *et al* found that serine 99, a putative phosphorylation site, in the Core was essential for infectious virion production [7]. In any event, the Core motif that is needed for interaction with the ESCRT components remains to be identified.

Ubiquitin modification of viral protein has been implicated in virion egress as well as in protein turnover. Indeed, the ubiquitin/proteasome system is required for the retrovirus budding machinery, since proteasome inhibition interferes with retroviral Gag polyprotein processing, release, and maturation. The ubiquitin modification of the HIV-1 p6 domain of Gag enhances TSG101 binding [12]. In the case of HCV Core, proteasomal degradation of the Core is mediated by two distinct mechanisms [33–36]. E6AP E3 ubiquitin ligase mediates ubiquitylation and degradation of the Core [34]. In contrast, proteasome activator PA28γ (11S regulator γ), an HCV Core-binding protein, is involved in the ubiquitin-independent degradation of the Core and HCV propagation [33,35,36]. However, little is known whether or not the ubiquitin modification of the Core might be involved in HCV egress like other enveloped viruses.

Finally, the identification of the site of viral particle assembly and budding is an intriguing issue. In case of HCV, at present, it is very difficult to visualize the HCV budding site in the infected cells by an electron microscopy. However, recent studies suggested that lipid droplets are an important cytoplasmic organelle for HCV production [4]. In this regard, Shavinskaya *et al.* demonstrated that

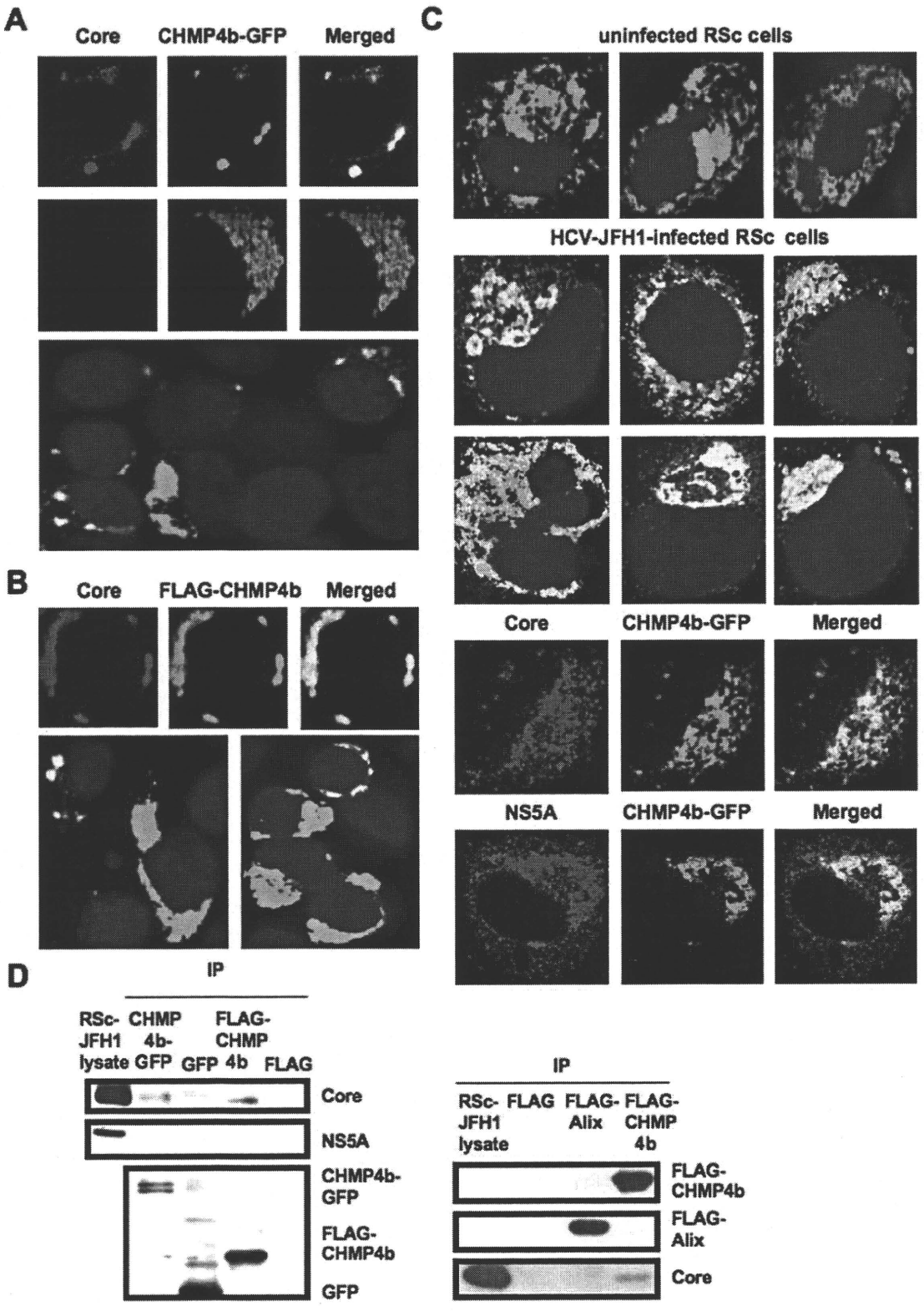

Figure 4. HCV Core interacts with CHMP4b. (A–C) HCV Core colocalizes with CHMP4b. 293FT cells cotransfected with 100 ng of pcDNA3/core (JFH1) and either 100 ng of pCHMP4b-GFP [39] (A) or pFLAG-CHMP4b [39] (B) were examined by confocal laser scanning microscopy. Cells were stained with anti-HCV Core and anti-FLAG polyclonal antibody and were then visualized with FITC (FLAG-CHMP4b) or Cy3 (Core). Images were visualized using confocal laser scanning microscopy. The right panels exhibit the two-color overlay images (Merged). Colocalization is shown in yellow. (C) The Core or NS5A partially colocalizes with CHMP4b in HCV-JFH1-infected RSc cells. RSc cells transfected with 100 ng of pCHMP4b-GFP were infected with HCV-JFH1. Cells were fixed 60 hrs post-infection and were then examined by confocal laser scanning microscopy as shown in panel (A). (D) HCV Core binds to CHMP4b. 293FT cells transfected with 4 μg of pCHMP4b-GFP, pEGFP C3 (Clontech), pcDNA3-FLAG, pcDNA3-FLAG-Alix or pFLAG-CHMP4b and RSc cells 5 days after inoculation of HCV-JFH1 at an MOI of 4 were lysed. The mixtures of these lysates were immunoprecipitated with either anti-FLAG or Living Colors A.v. monoclonal antibody (anti-GFP antibody), followed by immunoblot analysis using anti-HCV Core, anti-HCV NS5A, anti-FLAG, and/or Living Colors A.v. monoclonal antibody.
doi:10.1371/journal.pone.0014517.g004

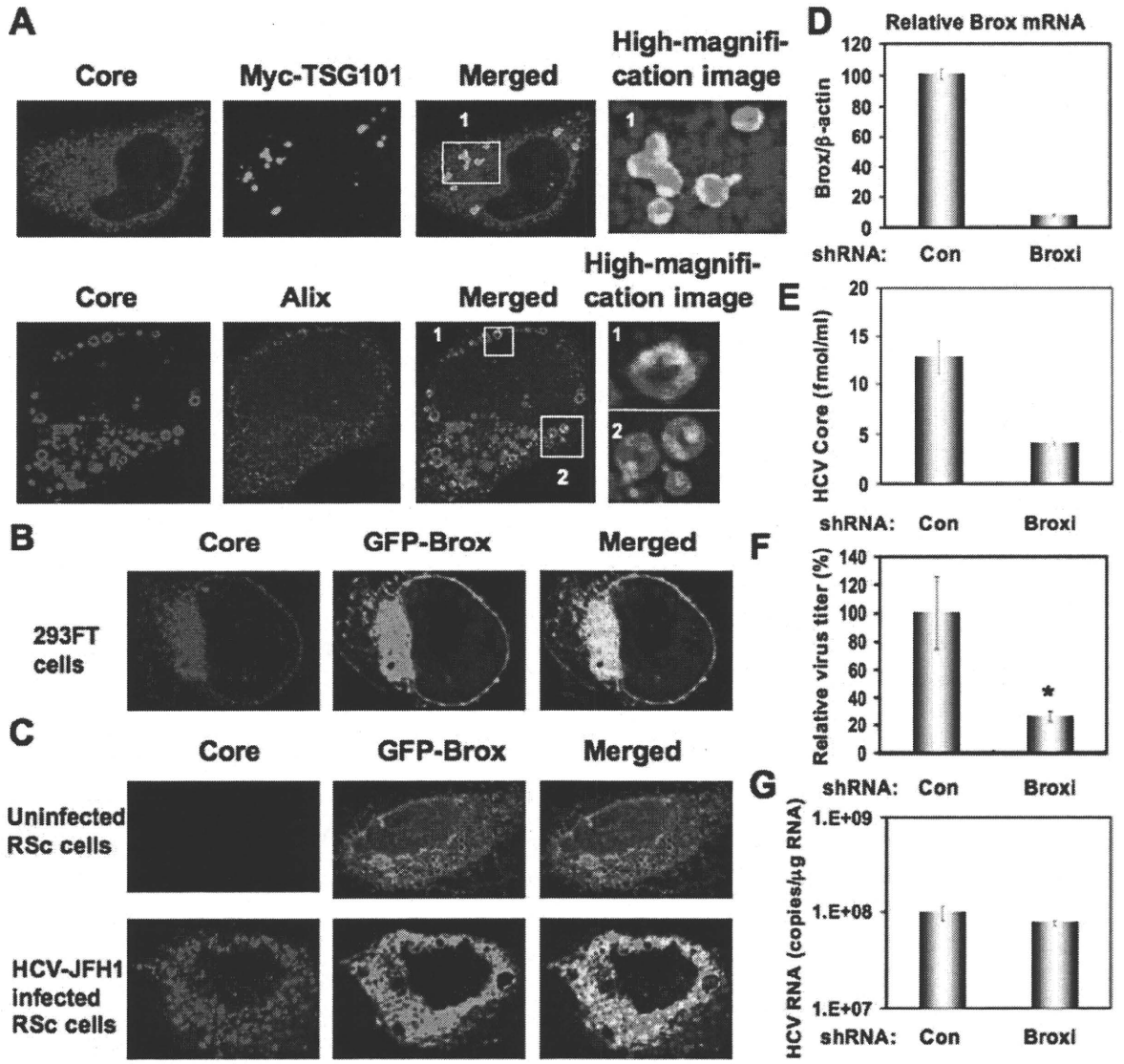

Figure 5. Brox is required for HCV life cycle. (A) Subcellular localization of Myc-tagged TSG101 in HCV-JFH1-infected RSc cells. RSc cells transfected with 100 ng of pBj-Myc-TSG101 [40] were infected with HCV-JFH1. Cells were fixed 60 hrs post-infection and were then examined by confocal laser scanning microscopy as shown in Fig. 3. High magnification image of area 1 is shown. Subcellular localization of endogenous Alix in HCV-JFH1-infected RSc cells 60 hrs post-infection. Cells were stained with anti-Alix and anti-HCV Core antibodies and were examined by confocal laser scanning microscopy. High magnification images of area 1 and area 2 are shown. (B) HCV Core partially colocalizes with Brox. 293FT cells cotransfected with 100 ng of pcDNA3/core (JFH1) and 100 ng of pmGFP-Brox^{WT} [27] were examined by confocal laser scanning microscopy. (C) The HCV Core partially colocalizes with Brox in HCV-JFH1-infected RSc cells. RSc cells transfected with 100 ng of pmGFP-Brox^{WT} were infected with HCV-JFH1. Cells were fixed 60 hrs post-infection and were then examined by confocal laser scanning microscopy. (D) Inhibition of Brox mRNA expression by the shRNA-producing lentiviral vector. Real-time LightCycler RT-PCR for Brox was performed as well as for β-actin mRNA in triplicate. Each mRNA level was calculated relative to the level in RSc cells transduced with a control lentiviral vector (Con) which was assigned as 100%. (E) The levels of HCV Core in the culture supernatants from the Brox knockdown RSc cells (Broxi) 72 hrs after inoculation of HCV-JFH1 were determined by ELISA. (F) The infectivity of HCV in the culture supernatants was determined by a focus-forming assay at 48 hrs post-infection. Experiments were done in triplicate and each virus titer was calculated relative to the level in RSc cells transduced with a control lentiviral vector (Con) which was assigned as 100%. Asterisks indicate significant differences compared to the control treatment. *$P<0.05$; **$P<0.01$. (G) The levels of intracellular genome-length HCV-JFH1 RNA in the cells used in (E) were monitored by real-time LightCycler RT-PCR.
doi:10.1371/journal.pone.0014517.g005

the lipid droplet-binding domain of the Core is a major determinant for efficient virus assembly [6]. The HCV Core induces lipid droplet redistribution in a microtubule- and dynein-dependent manner, since disrupting the microtubule network reduced the HCV titer, implicating transport networks in virus assembly and release [2]. Furthermore, Sandrin *et al.* reported that HCV envelope proteins localized to ESCRT-associated multivesicular body (MVB) [37]. Quite recently, Corless *et al.* have demonstrated that Vps4B and the ESCRT-III complex are required for HCV production [38]. Consistent with our findings, their dominant-negative forms of Vps4B and CHMP4B clearly suppressed HCV production. However, their dominant-negative forms of TSG101 and Alix failed to suppress the HCV production and they suggested that both TSG101 and Alix are unrelated to the HCV production. In contrast, we have demonstrated both TSG101 and Alix are also required for the infectious HCV

production by using shRNAs and siRNAs (Fig. 1). We may partly explain such discrepancy due to the difference of the methodology in our study utilized shRNAs and siRNAs instead of dominant-negative forms of TSG101 and Alix. Importantly, they demonstrated that the dominant-negative forms of Vps4B and CHMP4b did not affect the HCV RNA replication and the accumulation of intracellular infectious particles, suggesting that Vps4B and CHMP4b are unrelated to HCV RNA replication. Indeed, we have demonstrated that the ESCRT system is not required for the assembly of intracellular infectious HCV particles (Fig. 2E). Notably, we have demonstrated for the first time that HCV Core associated with CHMP4b (Fig. 4). Accordingly, we have also demonstrated that Brox, a CHMP4b binding protein, is required for HCV production (Fig. 5D–G). Taking together the past and present findings, we propose that the ESCRT system is involved in infectious HCV production after the HCV assembly that occurs on lipid droplets.

Acknowledgments

We thank D. Trono, R. Iggo, R. Agami, A. Takamizawa, and K. Shimotohno for pCMVΔR8.91, pMDG2, pSUPER, pRDI292, and anti-NS5A antibody, respectively. We also thank K. Abe for construction of pJRN/3-5B and T. Nakamura for his technical assistance.

Author Contributions

Conceived and designed the experiments: YA NK. Performed the experiments: YA MK. Analyzed the data: YA. Contributed reagents/materials/analysis tools: MM MI HD TW. Wrote the paper: YA NK.

References

1. Kato N, Hijikata M, Ootsuyama Y, Nakagawa M, Ohkoshi S, et al. (1990) Molecular cloning of the human hepatitis C virus genome from Japanese patients with non-A, non-B hepatitis. Proc Natl Acad Sci USA 87: 9524–9528.
2. Boulant S, Douglas MW, Moody L, Budkowska A, Targett-Adams P, et al. (2008) Hepatitis C virus core protein induces lipid droplet redistribution in a microtubule- and dynein-dependent manner. Traffic 9: 1268–1282.
3. Masaki T, Suzuki R, Murakami K, Aizaki H, Ishii K, et al. (2008) Interaction of hepatitis C virus nonstructural protein 5A with core protein is critical for the production of infectious virus particles. J Virol 82: 7964–7976.
4. Miyanari Y, Atsuzawa K, Usuda N, Watashi K, Hishiki T, et al. (2007) The lipid droplet is an important organelle for hepatitis C virus production. Nat Cell Biol 9: 1089–1097.
5. Shi ST, Polyak SJ, Tu H, Taylor DR, Gretch DR, et al. (2002) Hepatitis C virus NS5A colocalizes with the core protein on lipid droplets and interacts with apolipoproteins. Virology 292: 198–210.
6. Shavinskaya A, Boulant S, Penin F, McLauchlan J, Bartenschlager R (2007) The lipid droplet binding domain of hepatitis C virus core protein is a major determinant for efficient virus assembly. J Biol Chem 282: 37158–37169.
7. Murray CL, Jones CT, Tassello J, Rice CM (2007) Alanine scanning of the hepatitis C virus core protein reveals numerous residues essential for production of infectious virus. J Virol 81: 10220–10231.
8. Appel N, Zayas M, Miller S, Krijnse-Locker J, Schaller T, et al. (2008) Essential role of domain III of nonstructural protein 5A for hepatitis C virus infectious particle assembly. PLOS Pathog 4: e1000035.
9. Tellinghuisen TL, Foss KL, Treadaway J (2008) Regulation of hepatitis C virion production via phosphorylation of the NS5A protein. PLoS Pathog 4: e1000032.
10. Bieniasz PD (2006) Late budding domains and host proteins in enveloped virus release. Virology 344: 55–63.
11. Chen BJ, Lamb RA (2008) Mechanisms for enveloped virus budding: Can some viruses do without an ESCRT? Virology 372: 221–232.
12. Garrus JE, von Schwedler UK, Pornillos OW, Morham SG, Zavitz KH, et al. (2001) Tsg101 and vacuolar protein sorting pathway are essential for HIV-1 budding. Cell 107: 55–65.
13. Wakita T, Pietschmann T, Kato T, Date T, Miyamoto M, et al. (2005) Production of infectious hepatitis C virus in tissue culture from a cloned viral genome. Nat Med 11: 791–796.
14. Ariumi Y, Kuroki M, Abe K, Dansako H, Ikeda M, et al. (2007) DDX3 DEAD-box RNA helicase is required for hepatitis C virus RNA replication. J Virol 81: 13922–13926.
15. Ariumi Y, Kuroki M, Dansako H, Abe K, Ikeda M, et al. (2008) The DNA damage sensors, ataxia-telangiectasia mutated kinase and checkpoint kinase 2 are required for hepatitis C virus RNA replication. J Virol 82: 9639–9646.
16. Kuroki M, Ariumi Y, Ikeda M, Dansako H, Wakita T, et al. (2009) Arsenic trioxide inhibits hepatitis C virus RNA replication through modulation of the glutathione redox system and oxidative stress. J Virol 83: 2338–2348.
17. Ikeda M, Abe K, Dansako H, Nakamura T, Naka K, et al. (2005) Efficient replication of a full-length hepatitis C virus genome, strain O, in cell culture, and development of a luciferase reporter system. Biochem Biophys Res Commun 329: 1350–1359.
18. Ikeda M, Abe K, Yamada M, Dansako H, Naka K, et al. (2006) Different anti-HCV profiles of statins and their potential combination therapy with interferon. Hepatology 44: 117–125.
19. Ariumi Y, Kaida A, Hatanaka M, Shimotohno K (2001) Functional cross-talk of HIV-1 Tat with p53 through its C-terminal domain. Biochem Biophys Res Commun 287: 556–561.
20. Abe K, Ikeda M, Ariumi Y, Dansako H, Wakita T, et al. (2009) HCV genotype 1b chimeric replicon with NS5B of JFH-1 exhibited resistance to cyclosporine A. Arch Virol 154: 1671–1677.
21. Ariumi Y, Ego T, Kaida A, Matsumoto M, Pandolfi PP, et al. (2003) Distinct nuclear body components, PML and SMRT, regulate the trans-acting function of HTLV-1 Tax oncoprotein. Oncogene 22: 1611–1619.
22. Brummelkamp TR, Bernard R, Agami R (2002) A system for stable expression of short interfering RNAs in mammalian cells. Science 296: 550–553.
23. Bridge AJ, Pebernard S, Ducraux A, Nicoulaz AL, Iggo R (2003) Induction of an interferon response by RNAi vectors in mammalian cells. Nat Genet 34: 263–264.
24. Ariumi Y, Priscilla T, Masutani M, Trono D (2005) DNA damage sensors ATM, ATR, DNA-PKcs, and PARP-1 are dispensable for human immunodeficiency virus type 1 integration. J Virol 79: 2973–2978.
25. Naldini L, Blömer U, Gallay P, Ory D, Mulligan R, et al. (1996) In vivo gene delivery and stable transduction of non-dividing cells by a lentiviral vector. Science 272: 263–267.
26. Zufferey R, Nagy D, Mandel RJ, Naldini L, Trono D (1997) Multiply attenuated lentiviral vector achieves efficient gene delivery in vivo. Nat Biotechnol 15: 871–875.
27. Ichioka F, Kobayashi R, Katoh K, Shibata H, Maki M (2008) Brox, a novel farnesylated Bro1 domain-containing protein that associates with charged multivesicular body protein 4 (CHMP4). FEBS J 275: 682–692.
28. Chiou CT, Hu CCA, Chen PH, Liao CL, Lin YL, et al. (2003) Association of Japanese encephalitis virus NS3 protein with microtubules and tumor susceptibility gene 101 (TSG101) protein. J Gen Virol 84: 2795–2805.
29. Yi M, Ma Y, Yates J, Lemon SM (2007) Compensatory mutations in E1, p7, NS2, and NS3 enhance yields of cell culture-infectious intergenotypic chimeric hepatitis C virus. J Virol 81: 629–638.
30. Ma Y, Yates J, Liang Y, Lemon SM, Yi M (2008) NS3 helicase domains involved in infectious intracellular hepatitis C virus particle assembly. J Virol 82: 7624–7639.
31. Blanchard E, Hourioux C, Brand D, Ait-Goughoulte M, Moreau A, et al. (2003) Hepatitis C virus-like particle budding: Role of the core protein and importance of its Asp^{111}. J Virol 77: 10131–10138.
32. Klein KC, Dellos SR, Lingappa JR (2005) Identification of residues in hepatitis C virus core protein that are critical for capsid assembly in a cell-free system. J Virol 79: 6814–6826.
33. Moriishi K, Okabayashi T, Nakai K, Moriya K, Koike K, et al. (2003) Proteasome activator 28γ-dependent nuclear retention and degradation of hepatitis C virus core protein. J Virol 77: 10237–10249.
34. Shirakawa M, Murakami K, Ichimura T, Suzuki R, Shimoji T, et al. (2007) E6AP ubiquitin ligase mediates ubiquitylation and degradation of hepatitis C virus core protein. J Virol 81: 1174–1185.
35. Suzuki R, Moriishi K, Fukuda K, Shirakura M, Ishii K, et al. (2009) Proteasomal turnover of hepatitis C virus core protein is regulated by two distinct mechanisms: a ubiquitin-dependent mechanism and a ubiquitin-independent but PA28γ-dependent mechanism. J Virol 83: 2389–2392.
36. Moriishi K, Shoji I, Mori R, Suzuki R, Suzuki T, et al. (2010) Involvement of PA28gamma in the propagation of hepatitis C virus. Hepatology 52: 411–420.
37. Sandrin V, Boulanger P, Penin F, Granier C, Cosset FL, et al. (2005) Assembly of functional hepatitis C virus glycoproteins on infectious pseudoparticles occurs intracellularly and requires concomitant incorporation of E1 and E2 glycoproteins. J Gen Virol 86: 3189–3199.
38. Corless L, Crump CM, Griffin SD, Harris M (2010) Vps4 and ESCRT-III complex are required for the release of infectious hepatitis C virus particles. J Gen Virol 91: 362–372.
39. Katoh K, Shibata H, Suzuki H, Nara A, Ishidoh K, et al. (2003) The ALG-2-interacting protein Alix associates with CHMP4b, a human homologue of yeast Snf7 that is involved in multivesicular body sorting. J Biol Chem 278: 39104–39113.
40. Katoh K, Suzuki H, Terasawa Y, Mizuno T, Yasuda J, et al. (2005) The penta-EF-hand protein ALG-2 interacts directly with the ESCRT-I component TSG101, and Ca^{2+}-dependently co-localizes to aberrant endosomes with dominant-negative AAA ATPase SKD1/Vps4B. Biochem J 391: 677–685.

Published online 4 November 2010

Nucleic Acids Research, 2011, Vol. 39, No. 2 e7
doi:10.1093/nar/gkq966

High-level expression by tissue/cancer-specific promoter with strict specificity using a single-adenoviral vector

Yumi Kanegae*, Miho Terashima, Saki Kondo, Hiromitsu Fukuda, Aya Maekawa, Zheng Pei and Izumu Saito

Laboratory of Molecular Genetics, Institute of Medical Science, University of Tokyo, 4-6-1 Shirokanedai, Minato-ku, Tokyo 108-8639, Japan

Received March 26, 2010; Revised September 24, 2010; Accepted October 3, 2010

ABSTRACT

Tissue-/cancer-specific promoters for use in adenovirus vectors (AdVs) are valuable for elucidating specific gene functions and for use in gene therapy. However, low activity, non-specific expression and size limitations in the vector are always problems. Here, we developed a 'double-unit' AdV containing the Cre gene under the control of an α-fetoprotein promoter near the right end of its genome and bearing a compact 'excisional-expression' unit consisting of a target cDNA 'upstream' of a potent promoter between two *lox*Ps near the left end of its genome. When Cre was expressed, the expression unit was excised as a circular molecule and strongly expressed. Undesired leak expression of Cre during virus preparation was completely suppressed by a dominant-negative Cre and a short-hairpin RNA against Cre. Using this novel construct, a very strict specificity was maintained while achieving a 40- to 90-fold higher expression level, compared with that attainable using a direct specific promoter. Therefore, the 'double-unit' AdV enabled us to produce a tissue-/cancer-specific promoter in an AdV with a high expression level and strict specificity.

INTRODUCTION

Because tissue-specific promoters enable us to express a gene in a cell-type-specific manner *in vivo* or in a primary tissue culture, such promoters offer an attractive approach to studying the specific functions of a gene product in the tissues of experimental animals, such as in the brain where cells of different types are present together in the same region. The use of transgenic/knockout mice and adenovirus vectors (AdVs) are the most common approaches for utilizing these promoters. Among such promoters, those specific to malignant cells may be valuable for specific gene therapy or the diagnosis of cancer.

However, one drawback of such promoters is that their expression levels are much lower than those of a versatile promoter, such as the cytomegalovirus (CMV) immediate-early, CAG (1) or EF1α (2) promoters. For example, the α-fetoprotein (AFP) promoter, which is a relatively strong promoter among tissue-specific promoters, is reported to be ~500-fold less active than the CAG promoter (3), limiting its usefulness. Another important problem associated with the use of these promoters is that their specificity was often not sufficiently strict. One possible reason is that the excised segment of a specific promoter lacks the sufficient control of specific silencers and shows some 'basal level' of expression. In some cases, the lack of specificity might arise from the DNA elements surrounding the promoter, rather than the intrinsic character of the specific promoter (4,5). In human gene therapy using AdV, a strict specificity is critically important for safety as well as efficacy.

As one solution, we previously reported a 'double-infection' method (3), in which the virtual activity of AFP promoter was increased by about 50-fold while maintaining a strict specificity. With this method, two AdVs are infected simultaneously: one AdV contains a 'switch unit' consisting of Cre gene under the control of AFP promoter, and the other AdV bears a 'target unit' consisting of the CAG promoter,

*To whom correspondence should be addressed. Tel: +81 3 54495556; Fax: +81 3 5449 5432; Email: kanegae@ims.u-tokyo.ac.jp
Present addresses:
Saki Kondo, Cell Regulation Laboratory, Paterson Institute for Cancer Research, University of Manchester, Wilmslow Road, Manchester, M20 4BX, UK
Hiromitsu Fukuda, Japan Animal Referral Medical Center, 2-5-8 Kuji, Takatsu-ku, Kawasaki-shi, Kanawawa 213-0032, Japan

*lox*P, the stuffer sequence, second *lox*P, and a target cDNA, in that order. In non-hepatocarcinoma cells, the expression of the reporter cDNA remains turned off. However, in target hepatocarcinoma cells, AFP promoter in the switch unit of one AdV is turned on, leading to the production of Cre enzyme; this in turn leads to the excision of the stuffer sequence in the other AdV by Cre-mediated site-specific recombination, leaving the CAG promoter and the target gene connected only through a *lox*P sequence and enabling the strong expression of the target gene. Even when AFP promoter is weak and only a small quantity of Cre protein is produced, Cre can act as an enzyme multiple times, allowing most of the target AdV genomes to be processed eventually and accounting for the very high level of expression that can be obtained. The double infection method has been applied in numerous *in vivo* studies examining gene therapy for lung, colon and gastric cancers using the carcinoembryonic antigen promoter (6–10), for thyroid cancer using the thyroglobulin promoter (11), for hepatocellular carcinoma using AFP promoter (12), for prostate cancer using the prostate-specific antigen promoter (13) and for astrocytoma using the astrocytoma-specific promoter for GFAP (14). The method has also been applied in brain research using a modified, neuron-specific promoter of superior cervical ganglion 10 (15).

However, because the double-infection method uses two different AdVs simultaneously, controlling the infection is complicated and not often reproducible. Additionally, the toxicity and inflammation are at least doubled, compared with a single viral infection, for transducing the same amount of the target unit. Moreover, since a single cell infected with only one of the vectors does not produce any target protein, many such cells remain unused, causing a low expression as a result of dilution (12). Therefore, as a simpler, safer and more effective vector, an AdV bearing both the switch and the target unit simultaneously in a single genome is needed. However, the development of such an AdV has been regarded as being very difficult, since the sum of the lengths of both units exceeds the maximum length of the AdV genome. Furthermore, a leak in the expression of Cre can produce a large amount of stuffer-lacking AdV during vector preparation, causing severe non-specific expression. In addition, an enhancer of the potent promoter in the target unit may decrease the specificity of the specific promoter in the switch unit. Thus, a new vector is needed to solve these problems.

Here, we report the development and successful preparation of an AdV containing both units in a single genome. The vector, called a 'double-unit' AdV, possesses an extraordinary 'excisional-expression' structure and solves the aforementioned problems simultaneously, because the target unit of this vector lacks a stuffer sequence and because the target gene is expressed not from its genome, but from an excised circular DNA. The developed AdV shows a high level of expression (40- to 90-fold) while maintaining a very strict specificity.

MATERIALS AND METHODS

Cells and AdVs

The human embryo kidney cell line, 293 (16), constitutively expresses adenoviral E1 genes and supports the replication of E1-substituted AdV. HepG2 (17) and HuH7 (18) cells are human hepatocellular carcinoma cell lines that produce AFP. SK-Hep-1 (19) cells are a human hepatocellular carcinoma cell line that lack AFP production. HeLa cells, derived from cervical cancer, do not express AFP (20). The cell line CV1 is derived from African green monkey kidney. The AFP promoter used here was the (AB)2S6 AFP promoter (3). The EF1α promoter has been described previously (2). AxA2ANCre was described previously (3). AxLR14EL-AC, AxLR16EL-AC, AxLR16EFL, Ax-AC, AxNZ, AxLNZCAL, AxALNZCAL, AxA2AdsR and AxEFdsR are described for the first time in this work. AdVs described here were constructed using cosmid transfection (21). All the aforementioned viruses except for AxA2AdsR and AxEFdsR possessed E3 region with a 2.4-kb deletion, while the latter two viruses bore E3 region with the 1.9-kb deletion described in reference (21) (see 'Discussion' section). The switch unit was inserted at the *Sna*BI site (nt position 35 770), located 165-nt downstream from the right end of the adenovirus-5 (Ad5) genome. Because the standard Ad5 genome does not contain the *Sna*BI site, we generated a restriction site using nucleotide substitution, inserted a *Swa*I linker, and then cloned the switch unit. All the viruses were purified using a CsCl step gradient (22) and titrated using a method measuring 50% tissue culture infectious dose ($TCID_{50}$) (22); the viral particle: $TCID_{50}$ ratio was ~20:100, including double-unit viruses. The viral titer of all the AdV, including double-unit vectors was measured with $TCID_{50}$ using normal 293 cells.

Dominant negatives and shRNAs of Cre and isolation of Cre-suppressed 293 cells

dnCreRY was a dominant negative of Cre, where Arg173 and Tyr324 were mutated to Ala and Phe, respectively. pyCANCRYit2 is a plasmid expressing dnCreRY under the control of CAG promoter. The dnCreRY cDNA was excised as a *Sma*I-*Bgl*II fragment and inserted into pTrcHis2A (Invitrogen) between the *Ecl*36II and *Bgl*II sites under the *Escherichia coli* trc promoter (23). The *Bss*SI-*Sph*I fragment containing trc-dnCreRY was transferred upstream of the cos site of cosmid pAxLR16EL-AC and pAxLR14EL-AC, which were both derived from pAxcwit2 (21). The resulting cosmids were named ptdC-AxLR16EL-AC and ptdC-AxLR14EL-AC, respectively. shCreD (TA0493-4-D) was an shRNA of Cre, gatccGAAGCAACTCATCGATTGAtagtgctcctg gttgTCAATCGATGAGTTGCTTCtttttta (Cre sequences are in capitals), which efficiently suppressed Cre activity. TA0493-4-D was inserted under the human U6 promoter of plasmid pBAsi hU6 Pur (Takara Bio). The 293dnCreRY8 and 293shCreD13 were the best cell lines containing dnCreRY under the control of CAG promoter

and shCreD driven by human U6 promoter suppressing Cre activity among those tested, respectively.

To generate 293dnCreRY8, pBCANCRYSAPur was constructed, expressing dnCreRY under the control of the CAG promoter and the puromycin-resistant (Pur^R) gene under the control of the SV40 early promoter (Figure 5a). To generate 293shCreD13, pBSAPurhU6shCre was constructed, expressing one of the short-hairpin (sh) RNAs against Cre under the control of the human U6 promoter (Takara Bio) and the Pur^R gene identical to that expressed by pBCANCRYSAPur (Figure 5b). Ten micrograms of each plasmid DNA were transfected into 293 cells using Transfast^R (Promega). Two days after transfection, puromycin was added at a concentration of 2.5 μg/ml. We selected the cell line that most efficiently caused a reduction of Cre activity for the simultaneous transfection in Cre-expressing and target pCALNLG plasmids (24).

Preparation of total cell DNA for restriction-enzyme digestion and for real-time PCR

Infected cell DNA was prepared on a 24-well plate as previously described (25) with some modifications: the cells were suspended in 0.4 ml of TNE-PK [50 mM Tris–HCl (pH 8), 100mM NaCl, 10 mM EDTA, 100 mg/ml proteinase K], followed by the addition of SDS (final 0.1%). After incubation at 55°C for 2 h, the mixture was extracted once with phenol–chloroform and once with chloroform, and precipitated with 1 or 1.5 volumes of ethanol at −20°C for >1 h and then washed once with 70% ethanol. The pellet was dissolved with 50 ml of TE containing 20 mg/ml RNase A and stored at −20°C. This DNA was sufficient not only for real-time PCR but also for gel electrophoresis to observe the structure of the AdV genome.

To detect viral DNA, total DNA extracted from AxLR16EL-AC-infected, Cre-suppressed 293 cells in a 24-well plate was digested with *Bmg*BI. The *Bmg*BI recognition sequence, CACGTG, contains a -CG- dinucleotide, which is mostly methylated in the mammalian genome and cannot be cleaved by a restriction enzyme, while replicating adenoviral DNA is not methylated and can be cleaved. Consequently, restricted patterns of only adenoviral DNA can be seen.

Quantification of AdV transduction efficiency and expressed RNA

Total cell DNA was prepared as described above. Real-time PCR was performed to detect the adenovirus genome using a probe for the pIX gene, and human chromosome was simultaneously detected using a probe for the β-actin gene or the ornithine transcarbamylase (OTC) gene. The threshold cycle (cT) values were obtained. All the probes used in the study are shown in Table 1. The cT value of the AdV was corrected according to that for the human chromosome probe. The sequences of these probes were shown in Table 1. Infected cell RNA was prepared using the RNeasy protect mini kit (Qiagen) according to the manufacturer's protocol. To prepare the cDNA, the TaqMan Reverse Transcriptase Reagent kit (Applied BioSystems) was used. The sequences of the dsRed probes are shown in Table 1. The 18S rRNA primer used in the study were Ribosomal Eukaryotic 18S rRNA kit (Applied BioSystems).

Table 1. Sequences of probes used in real-time PCR

Probe[a]	Primer sequences[b]
AdV-1	F: TGTGATGGGCTCCAGCATT
	P: ATGGTCGCCCCGTCCTGCC
	R: TCGTAGGTCAAGGTAGTAGAGTTTGC
hOTC-1	F: CCACTACAAAATAAAGTGCAGCTGAA
	P: CCGTGACCTTCTCACTCTAAAAAACTT
	R: CTGATAGCCATAGCATATATTTAATTTCTTCTC
β-Act-1	F: CTCGCAGCTCACCATGGAT
	P: ATGATATCGCCGCGCTCGTCGT
	R: ATGCCGGAGCCGTTGTC
dsRed-1	F: GCAGCTGCCCGGCTACT
	P: CGTGGACTCCAAGCTGGACATCACCT
	R: CGATGGTGTAGTCCTCGTTGTG

18S rRNA primers used were Ribosomal Enkaryotic 18S rRNA kit (Applied BioSystems).
[a]Name of the probes. Reporters used were FAM except β-Act-1 (VIC reporter).
[b]F, forward primer; P, probe; R, reverse primer. Real-time PCR was purchased from Applied BioSystems.

To examine the expressed dsRed RNA, the cells were infected with AdV and total DNA and the total RNA was extracted. From the total DNA, the amounts of AdV genome and β-actin gene were simultaneously quantified using real-time PCR and the ratio of AdV genome per cell was obtained. Similarly, from the total RNA, the amounts of dsRed RNA and 18S-rRNA (the correction standard) were quantified using reverse transcription and real-time PCR, and the ratio of dsRed RNA to 18S-rRNA was obtained. Based on these results, the ratio of the dsRed RNA level between the two cell lines was calculated.

Detection of expressed fluorescence

To evaluate the different EF1α promoter versions, the cells were washed twice with Hank's balanced salt solution 3 days after transfection, and the intensity of GFP fluorescence was quantified using Fluoroskan Ascent FL (Labsystems) (26). Cells infected with AxLR16EL-AC and AxLR14EL-AC were sorted using dsRed fluorescence using FACS (FACSCalibur, Becton-Dikinson). The dsRed fluorescence was also measured using Ascent fluorescent meter. To calculate the relative strengths among the various promoters, the steady-state level of the expressed dsRed RNA together with the dsRed DNA in the AdV genome in infected cells was quantified using a real-time PCR (Prism 7000, Applied Biosystems), and the former value was divided by the latter.

RESULTS

Structure of 'double-unit' vector containing 'excisional-expression' unit

The structure of the 'double-unit' AdV vector AxLR16EL-AC is shown in Figure 1. This vector is a

first generation AdV containing the switch unit inserted near the right end of the adenovirus genome (27) (denoted in this paper at the E4 position) and the target unit inserted in the E1 region. Since the adenovirus genome can be packaged into a capsid up to ~105% of, or 2 kb more than, the wild-type genome size (28), it was impossible to generate an AdV containing both the switch and the target units using a typical construction strategy because of over-sizing. Therefore, to shorten the total length of the units, an 'excisional-expression' structure was adopted for the target unit. Although a typical target unit for conditional expression possesses (in order) the potent promoter, *lox*P, a stuffer sequence, a second *lox*P, cDNA and polyadenylation sequences (poly(A)), the excisional-expression unit lacks a stuffer sequence and instead consists of (in order) the right *lox*P, dsRed cDNA, poly(A), EF1α promoter and the left *lox*P (Figure 1, Target unit on AxLR16EL-AC). Notably, the dsRed cDNA is located not downstream, but 'upstream' of the EF1α promoter and, therefore, dsRed expression is turned off in the initial structure because AFP promoter does not function in non-hepatocarcinoma cells. However, once the AdV infects a hepatocarcinoma cell, AFP promoter is turned on and Cre enzyme is produced. Consequently, the expression unit of dsRed—EF1α promoter with one *lox*P is 'excised' as a circular molecule (Figure 1, middle), and the dsRed cDNA is now located downstream of the EF1α promoter, turning its expression on. At the same time, an AdV genome with one *lox*P is produced (Figure 1, lower, AxL-AC).

To minimize the genome size of the double-unit AdV: (i) a 0.55-kb section of the E3 region was deleted (see 'Discussion' section). In addition (ii) the EF1α promoter was shortened from an original length of 2.1 kb to lengths of 1.6 and 1.4 kb (named 16EF and 14EF, respectively). Unexpectedly, both the 16EF and 14EF promoters showed higher activity levels than the original EF1α promoter (Figure 2). As well; (iii) the 0.6-kb rabbit β-globin poly(A) sequence was truncated to 0.3 kb up to *Nde*I site. In addition to the size limitation, the double-unit AdV possesses several features that enable a very strict specificity (see Discussion section). As an improvement, the poly(A) sequence of 137 nt derived from the SV40 early region (*Hpa*I-*Bam*HI) was added in front of the dsRed cDNA plus the right *lox*P on the target unit (Figure 1, upper) based on the results of the following experiments. We constructed three AdVs containing the *lac*Z DNA tagged with the nuclear localization signal [NLacZ (3)] and their structures are shown in Figure 3a. CV1 cells were infected with each of these AdVs at multiplicity of infection (MOI) of 50 and, three days later, the *lac*Z expression of the infected cells was detected with X-gal staining. When cells were infected with AxNZ containing promoterless NLacZ (Figure 3a, top), weak but significant background expression was observed in most of the cells (Figure 3b, lower left); such expression was not observed in mock-infected cells (Figure 3b, upper left). When cells were infected with AxLNZCAL containing an excisional expression unit lacking the poly(A) in front of the NLacZ plus *lox*P (Figure 3a, middle), significant expression was observed (Figure 3b, upper right) and the expression level was much higher than that using AxNZ (lower left). We speculate from these results that a weak cryptic promoter may present upstream of the NLacZ and be activated by the enhancer of CAG promoter downstream of the NLacZ. Nevertheless, using AxALNLZCAL containing the excisional expression unit possessing poly(A) in front of NLacZ DNA plus *lox*P (Figure 3a, bottom), the background expression was almost disappeared (Figure 3b, lower right). The result showed that the inserted poly(A) sequence effectively reduced the background expression. The results were confirmed in the transfection experiments using the cosmids containing the full-length AdV genome (data not shown). Finally, we attempted to construct two AdVs, AxLR16EL-AC (104.9% of wild-type adenovirus genome) and AxLR14EL-AC (104.4%) containing the 16EF and 14EF promoters, respectively. The genome sizes of both AdVs were under the size limit.

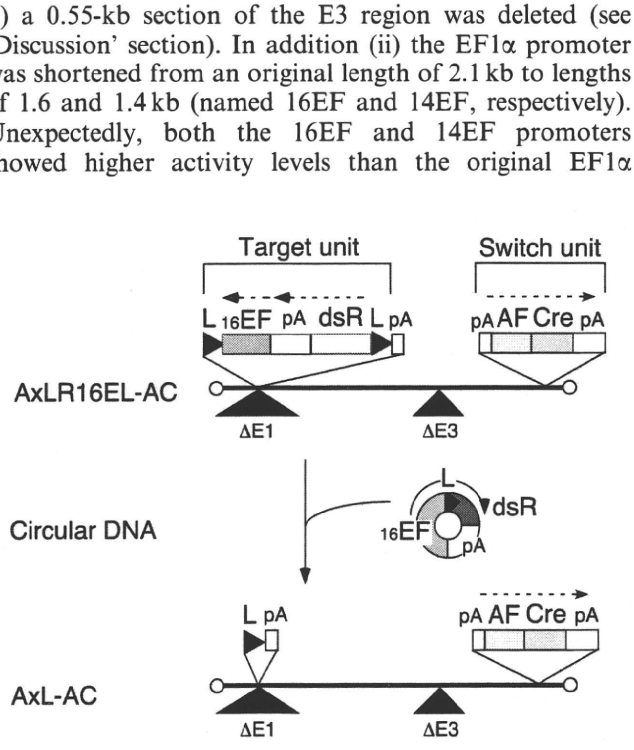

Figure 1. Structure of double-unit AdV and generation of expressing circular DNA. L, *lox*P; 16EF, shortened EF1α promoter; pA, poly(A) sequence; dsR, dsRed cDNA; AF, AFP promoter; Cre, nuclear localization signal-tagged Cre cDNA.

Leak expression of Cre both in *E. coli* and in 293 cells hampers the preparation of double-unit AdVs

Unexpectedly, during the construction of cosmids containing either AxLR16EL-AC or AxLR14EL-AC DNA (Figure 4a, dnCreRY –), we observed the co-generation of cosmids lacking the sequences between the two *lox*Ps (Figure 4b). The 2.5- and 2.7-kb bands (Figure 4c, lane 3) showed the presence of both cosmid DNA containing the AxL-AC genome and the excised circular DNA molecule, respectively. Judging from the intensities of the bands, the AxL-AC DNA accounted for ~15–20% of the midi-preparation (23) of *E. coli*. Thus, Cre must be expressed during cosmid preparation in *E. coli* DH5α despite the absence of an obvious *E. coli* promoter in the cosmid: the ampicillin promoter was present, but in the opposite orientation and ~20 kb away. Although the AxL-AC cosmid DNA was detected only faintly in the DNA of

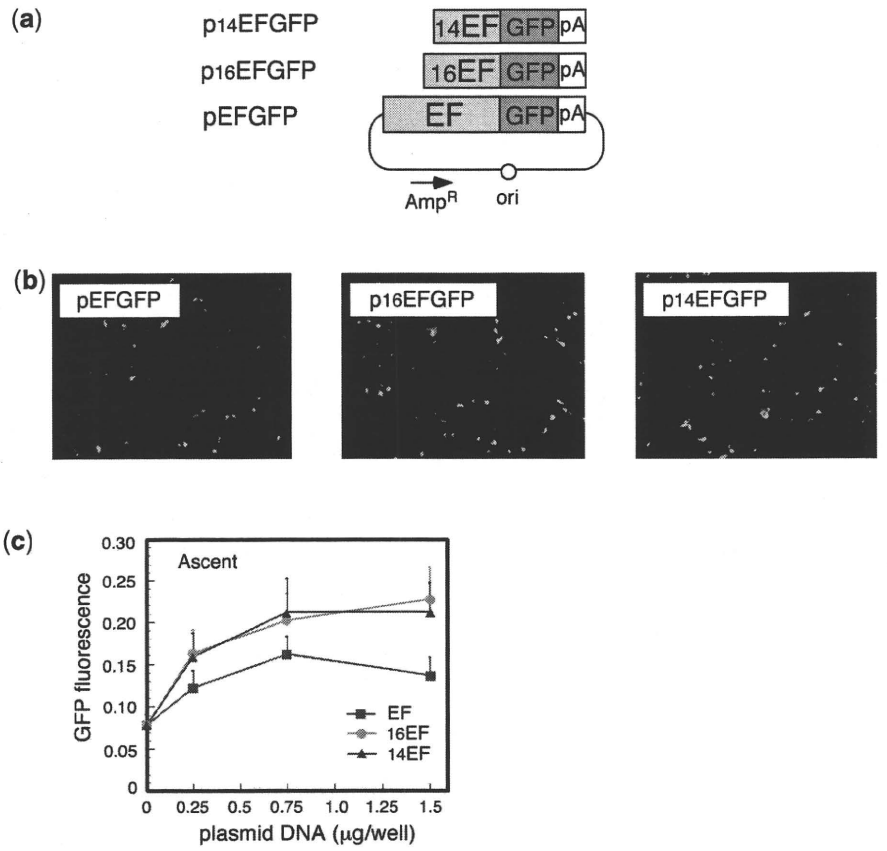

Figure 2. Expression of truncated EF1α promoter. (**a**) Structure of the plasmids expressing GFP under truncated EF1α promoter. The original EF1α promoter is 2.1-kb long. The 5′-end of 16EF was the *Ppu*MI site and that of 14EF was the *Blp*I site. (**b**) Images obtained using fluorescent microscopy. (**c**) Fluorescence measured using a fluoroscan plate reader. Vertical axis showed florescence in arbitrary unit; $n = 4$.

the mini-preparation (lane 2), it appeared to accumulate over time.

Furthermore, after the transfection of the cosmid DNA containing AxLR16EL-AC into 293 cells, all 12 of the viral clones that were generated were not the target virus, but apparently an AxL-AC virus. And three out of 18 viral clones derived from AxLR14EL-AC-containing cosmid DNA were mixtures of AxLR14EL-AC and AxL-AC viruses, while the other 15 clones were apparently pure AxL-AC virus (data not shown). These results showed that AFP promoter, which is thought to be inactive in non-hepatocellular 293 cells, certainly produced Cre in an amount sufficient to recombine the *lox*Ps on the AdV genome. This result probably occurred because even if the AFP promoter was strictly regulated, the AdV genome containing the switch unit of AFP promoter and Cre was amplified for 100 000 copies in one 293 cell and, consequently, an effective amount of Cre would be produced. Therefore, because of the leakage of Cre expression in both *E. coli* and 293 cells, double-unit vectors could not be prepared using conventional methods.

Successful suppression of leak expression of Cre using a dominant-negative of Cre and shRNA against Cre

To suppress the leak expression of Cre in *E. coli*, several dominant-negatives of Cre containing two amino acid mutations at the active center of Cre enzyme were constructed; dnCreRY, the dominant-negative that most efficiently suppressed Cre activity among those tested in co-transfection assays with a target plasmid, was then selected. Next, we constructed an expression unit producing dnCreRY under the control of the *trc* promoter of a *lac* operon system, and this unit was inserted into the cosmids containing AxLR16EL-AC and AxLR14EL-AC DNAs (Figure 4a, dnCreRY +). In the midi-preparation of this AxLR16EL-AC cosmid, neither the recombined AxL-AC-derived band nor the excised circular DNA molecule was detected with IPTG induction (Figure 4c, lane 7), showing that the production of dnCreRY successfully suppressed the leak expression of Cre in *E. coli*. Interestingly, since an apparent complete suppression was also observed without IPTG induction (lane 6), dnCreRY produced by the basal activity of the *trc* promoter was sufficient to suppress the leak expression of Cre effectively. Therefore, the problem of the leak expression of Cre in *E. coli* was solved.

To suppress the leak expression of Cre during AdV preparation in 293 cells, a plasmid expressing dnCreRY and a puromycin-resistant (PurR) gene (Figure 5a, upper) was transfected into 293 cells and the cell line 293dnCreRY8 was established; this cell line suppressed Cre activity the most efficiently. Virus clones were

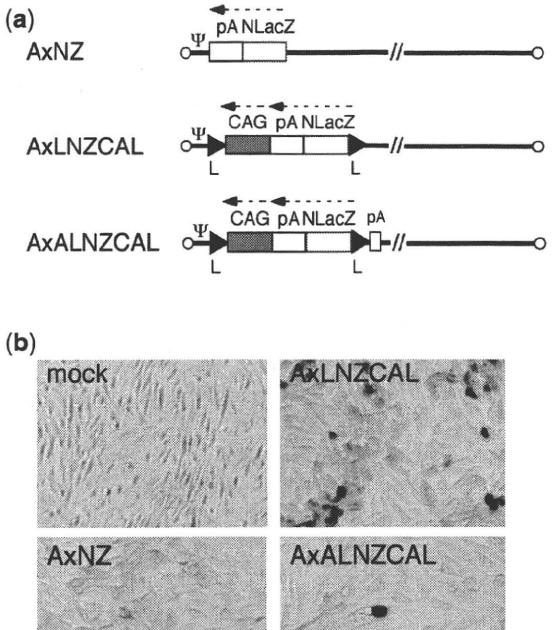

Figure 3. Suppression of the background expression by adding poly(A) sequence in front of *lacZ* DNA. (**a**) Structure of AdVs. (top) AxNZ contains the promoterless *lacZ* DNA; (middle) AxLNZCAL contains the excisional expression unit lacking poly(A) sequence in front of *lacZ* DNA plus right *lox*P; (bottom) AxALNZCAL contains that unit possessing poly(A) sequence in front of *lacZ* DNA plus right *lox*P. NlacZ, *lacZ* DNA tagged with NLS; Ψ, adenovirus packaging sequences; CAG, CAG promoter. The other representations are the same as in Figure 1. (**b**) Reduction of the 'background' expression observed using the promoterless *lacZ* DNA caused by addition of the poly(A) sequence. The infected CV1 cells were stained by X-gal. Very few dark-stained cells were observed in panels AxNZ (lower left) and AxALZCAL (lower right); the origin of these cells were unknown but possibly similar to those observed in Figure 7b and e.

obtained by transfecting linearized AxLR16EL-AC DNA, and the digestion of the viral genome with *Bmg*BI yielded a 1.8-kb band from an intact AxLR16EL-AC virus and a 1.4-kb band from a processed AxL-AC virus (Figure 5c). The 293dnCreRY8 cells did not produce pure AxLR16EL-AC virus, but instead produced mixtures of AxLR16EL-AC and AxL-AC (Figure 5a, lower, lanes 1, 3, 4 and 6) or mostly AxL-AC (lanes 2 and 5). Therefore, the suppression of Cre activity in the 293dnCreRY8 cells was not complete.

Meanwhile, several sh RNAs against Cre were constructed and screened, and shCreD was identified. Then, a plasmid expressing shCreD and PurR (Figure 5b, upper) was transfected into 293 cells, and the cell line 293shCreD13 was established. Unlike 293dnCreRY8, 293shCreD13 yielded mostly viral stocks of apparently pure AxLR16EL-AC virus (Figure 5b, lower, lanes 2, 3, 4 and 5), though some stocks were mixtures of both viruses (lanes 1 and 6). The AxLR16EL-AC virus in the apparently pure stocks was amplified in 293shCreD13 cells. To examine the 'leaky' expression level of Cre during the production of the double-unit vector in 293shCreD13 cells, an aliquot of AxLR16EL-AC viral stock was used to infect 293shCreD13 cells; then, to detect the viral genome, the total cell DNA was digested with *Bmg*BI. The 1.4-kb band produced by Cre recombination was not detected up to and including the third stock (data not shown) but, when the fourth stock purified using CsCl ultracentrifugation was examined, observed were the bands showing that the ratio of intact AxLR16EL-AC and 'leaked' AxL-AC was ~10:1 (Figure 5b, lower right). Of note, contamination with the AxL-AC virus does not cause any non-specific expression because Cre-processed AxL-AC virus does not contain an expression unit (Figure 1, bottom). An important point is that to prepare a double-unit AdV, the selection of an apparently

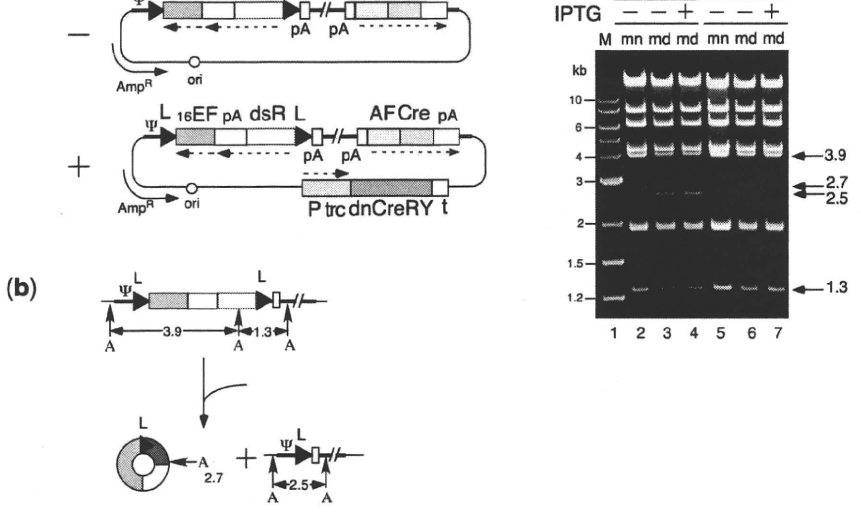

Figure 4. Leak expression of Cre in *E. coli*. Representations are the same as in Figure 1 unless otherwise stated. (**a**) Structure of cosmid generating double-unit AdV and expressing dnCreRY. Ψ, adenovirus packaging sequences; P trc, trc promoter; t, terminator. (**b**) Generation of Cre-processed molecules. A, *Ahd*I site. (**c**) Detection of Cre-processed molecules. M, 1-kb ladder marker; mn, mini-preparation; md; midi-preparation. The bands of 2.7 and 2.5 kb represent the generated circular DNA and Cre-processed DNA, respectively.

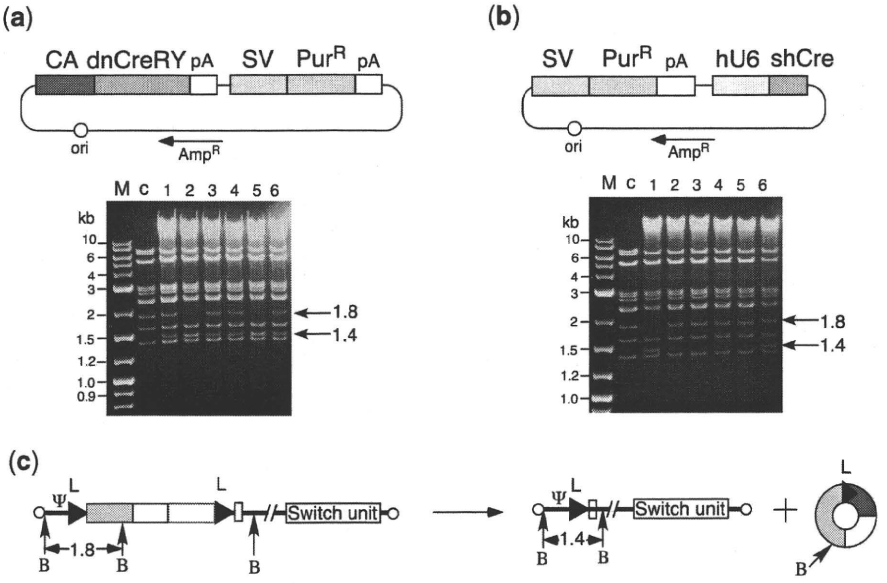

Figure 5. Establishment of 293 cell lines suppressing Cre activity. (**a**) Structure of plasmids expressing dnCreRY (upper) and DNA restriction pattern of double-unit viral clones produced in 293dnCreRY8 cells (lower). CA, CAG promoter; SV, SV40 early promoter; Pur^R, puromycin-resistant gene. The other representations are the same as in Figure 1. M, 1-kb ladder marker; c, restriction pattern of AxLR16EL-AC-containing cosmid DNA, presenting as a 1.8-kb band. (**b**) Structure of plasmids expressing shCre (upper) and DNA-restriction pattern of double-unit virus DNA of double-unit viral clones produced in 293shCreD13 cells (lower). hU6, human U6 promoter. P, purified/fourth stock was infected. The other representations are the same as in (a). (**c**) Generation of AxL-AC. B, *Bmg*BI site. The other representations are the same as in Figure 1. The presence or absence of circular 2.7-kb DNA was not clear in the gels of (a) and (b) because of the viral-derived bands of 2.9, 2.7 and 2.6 kb, but the circular DNA was hardly detected in the other experiment (data not shown). This result suggests that the production of the circular molecule occurs just after transfection and is consistent with the result that AxLR16EL-AC was stable up to the fourth stock.

Table 2. The viral titers of double-unit virus and the sprit viruses

Viruses[a]	Cells	Titers[b] ($TCID_{50}$)
AxLR16EL-AC	293shCreD13	1.1×10^{10}
AxLR16EL	Normal 293	4.7×10^{11}
Ax-AC	Normal 293	7.6×10^{10}

[a]The structure of AxLR16EL-AC is shown in Figure 1. The structures of split viruses, AxLR16EL and Ax-AC were shown in Figure 7a.
[b]Forth, purified viral stocks used in all experiments in this work.

pure first virus stock lacking AxL-AC as shown in Figure 5b, lower left, may be essential (see 'Discussion' section).

The 293shCreD13 cells grew well, similar to normal 293 cells, and the double-unit viruses were apparently able to proliferate in 293shCreD13 cells as well as normal E1-deficient AdV in 293 cells. Table 2 shows the titers of the double-unit virus AxLR16EL-AC produced in 293shCreD13 cells and of the split viruses shown in Figure 7a produced in normal 293 cells, all of which were used in this work. The titer of the double-unit virus was sufficiently high, though it was lower than those of the split viruses. One possible reason may be that the genome size of the former is near the upper limit. The AxLR14EL-AC virus was similarly prepared, and AxL-AC virus contamination was not detected in the third stock (data not shown).

The third viral stocks of double-unit virus without CsCl purification produced low but not negligible levels of non-specific dsRed expression when infected in HeLa cells (data not shown). Importantly, however, a viral preparation that was purified using a CsCl step gradient (22) did not produce any non-specific expression (see 'Discussion' section). Therefore, double-unit AdVs prepared in 293shCreD13 and purified using a CsCl step-gradient enabled the creation of viral stocks with a very strict specificity.

High-efficiency and very strict expression using double-unit AdV

The AxLR16EL-AC virus (at MOI of 5) was used to infect various cell types including HeLa (derived from non-liver carcinoma), SK-Hep1 (hepatocarcinoma-derived, non-producer of AFP), HuH-7 and HepG2 (hepatocarcinoma-derived producer of AFP). On day 3, high-level expressions of dsRed were observed in the infected HuH-7 and HepG2 cells (Figure 6h and k). Fluorescence-activated cell sorter (FACS) analyses showed that ~86 and 92% of these cells expressed detectable levels of dsRed, respectively (Figure 6i and l). In contrast, only one or two cells in a field of HeLa or SK-Hep1 cells expressed detectable levels of dsRed (Figure 6b and e), showing that the expression specificity of this vector was very strict. The FACS analyses confirmed that only 0.7 and 0.5% of the respective cells expressed detectable dsRed (Figure 6c and f). The results of dose-dependent experiments for all four cell lines confirmed the specificity of expression (Supplementary Figure S1).

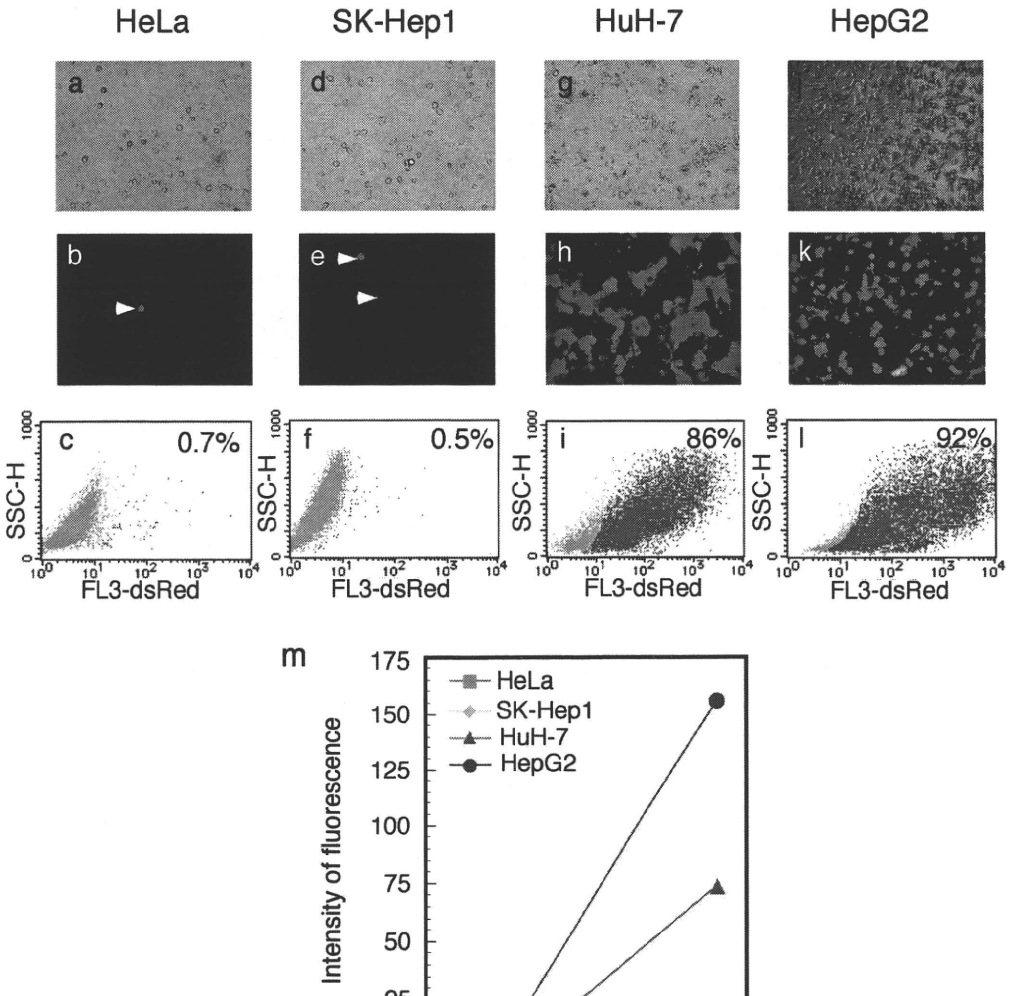

Figure 6. Specific and high-level expression of dsRed by AFP promoter using double-unit virus. Cells were infected with AxLR16EL-AC at MOI 5. (**a–c**) HeLa; (**d–f**) SK Hep-1; (**g–i**) HuH-7; (j, k and l) HepG2. (a, d, g and j) Phase-contrast microscopic views. (b, e, h and k) Images obtained using fluorescent microscopy. The arrow heads show exceptional cells with non-specific fluorescence. (c, f, i and l) FACS analysis of dsRed-expressing cells. SSC-H, side scattered light, high flow rate. (m) Dose responses of dsRed expression in the infected cells.

The dsRed expression was quantified using FACS by measuring the total sum of all cell fluorescence. The results showed that the ratio of the expressed mean fluorescence among the HeLa:SK-Hep1:HUH-7:HepG2 at MOI 5 in Figure 6c, f, i and l was 0.7:1:36.6:77.4, showing that the level of 'leaked' expression in the total cell population of AFP-negative cells compared with that in the AFP-positive cells was ~40 to 80 times less. The results of dose-dependent experiments are shown in Figure 6m. These results showed a very high expression and a strict specificity of this vector. Parallel to these FACS experiments, the transduction efficiency of the AdVs was measured by examining aliquots of all the four cell lines using real-time PCR as described in 'Materials and methods' section. The results indicated that the ratio of transduction efficiencies among HeLa, SK-Hep1, HuH-7 and HepG2 were 1.3:1:1.2:7.6, showing that the number of transduced AdV genomes present was almost the same for the first three cells. Therefore, these results confirmed very strict specificity of this vector for HeLa and SK-Hep1 cells. Meanwhile, HepG2 cells reproductively showed exceptionally high transduction efficiency. This seemed to be associated with the result that HepG2 showed much higher expression levels than HuH-7 cells (Figure 6m, at MOIs 1.7 and 5). Therefore, the very high expression level of HepG2 was partly explained by its exceptionally high transduction efficiency.

To examine the specificity of the double-unit vector, total RNA and DNA were extracted from AxLR16EL-AC-infected SK-Hep1 (AFP-negative) and HuH-7 (AFP-positive) cells. The amounts of expressed

dsRed RNAs and the transduced AdV genome were measured using real-time PCR as described in the Materials and methods section. The ratio of the dsRed RNA level corrected according to the transduced AdV genome between the two cell lines was calculated. The result showed that the dsRed RNA ratio of HuH-7 and SK-Hep1was 42.0:1, correlating well with the quantification of dsRed expression using FACS analyses. Identical experiments were performed using a control AdV AxCAdsRed expressing dsRed under the control of the CAG promoter instead of the double-unit vector. The result showed that the RNA ratio corrected according to the viral DNA amount between HuH-7 and SK-Hep1was 1.38:1, indicating that the activity of the CAG promoter was similar in both cell lines. These results indicated that the 'leak' level of the double-unit vector in the SK-Hep1 cells, compared with that in the HuH-7 cells, was ~1/40th of the expression level of HuH-7 cells (or 1/30th, based on of the CAG promoter control), demonstrating that the background level of double-unit vector in AFP-negative cells was again very low.

To examine the effect of combining the switch unit and the target unit into a single genome, we newly constructed two AdVs: AxLR16EL, containing only the target unit (Figure 7a, first), and Ax-AC, containing the switch unit at the E4 position (Figure 7a, second), as in AxLR16EL-AC. Then, the expression of the double-unit vector (AxLR16EL-AC) and the double infection of split viruses containing the excisional expression unit (AxLR16EL + Ax1AC) was examined using dsRed fluorescence. The double-unit vector showed a much higher fluorescence level than the double-infection method, as observed under a fluorescent microscope (Figure 7b). And the quantitative measurement of dsRed fluorescence showed that the former method produced 3.3-fold more dsRed protein than the latter method using an MOI of 13 (Figure 7c). The reason that the expression level was higher than that of the split viruses appears to be not only because the amount of the target virus was one half of the same total dose of the viruses, but also because in many cells, the split two vectors were not infected simultaneously or did not produce a sufficient amount of Cre during five days.

The steady-state levels of expressed dsRed RNA measured using real-time PCR in HuH-7 cells were compared with the direct expression under the control of AFP promoter (AxA2AdsR, Figure 7a), a double-unit vector (AxLR16EL-AC), a double-infection of split viruses (AxLR16EL + Ax-AC), and the expression under the control of EF1α promoter (AxEFdsR, Figure 7a) (Table 3). On Day 3, the double-unit vector expressed ~40-fold more dsRed RNA than the direct expression under the control of AFP promoter. Meanwhile, the double infection of split viruses (AxLR16EL + Ax-AC) expressed dsRed RNA at a level only 1/4th of that expressed by the double-unit vector, confirming the expression results (Figure 7c). Because the dsRed RNA expressed by the EF1α promoter (AxEFdsR) in HuH-7 cells was 480-fold higher than the direct expression of AFP promoter, the double-unit vector utilized ~1/10th of the EF1α promoter activity on day 3. However, on day 4, the

Table 3. Steady-state levels of expressed dsRed RNA in HuH-7 cells

AdV[a]	Ratio[b]
AxA2AdsR	1
AxLR16EL-AC	41
AxLR16EL + Ax-AC	10
AxEFdsR	480
AxLR16EL-AC (day 4)	91

Each experiment was performed twice to confirm the reproducibility; typical data are shown. The genome structures of the above viruses are shown in Figures 1 and 7a.
[a]HuH-7 cells were infected with each AdV at a MOI of 30. In the double infection, an MOI 15 of each virus was used.
[b]For each condition, the expressed dsRed RNA measured using real-time PCR was divided by the value obtained using the AxA2AdsR virus.

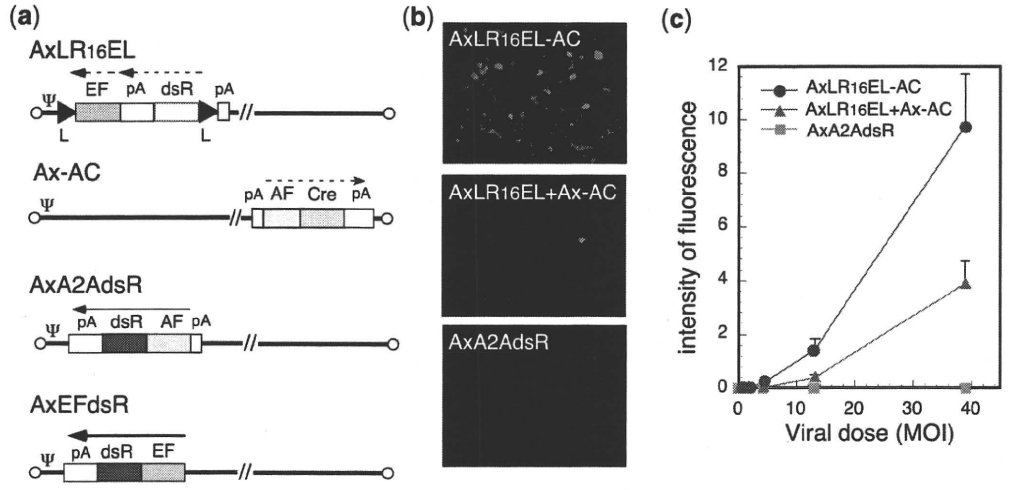

Figure 7. Simultaneous excisional expression in HuH-7 cells using double-infection method. (**a**) Structure of AdVs. The representations are the same as in Figure 1. (**b**) Images obtained using fluorescent microscopy. (**c**) Fluorescence measured using a fluoroscan plate reader.

expression of dsRed RNA reached ~90-fold when using the double-unit vector (Table 3); because such an increase in expression on later days was often observed in other double-unit experiments (data not shown), this result can likely be explained by the weak AFP promoter, since the very small amount of expressed Cre likely required a long time to process the target unit.

DISCUSSION

We developed a 'double-unit' AdV bearing an 'excisional-expression' structure and established a preparation method for this AdV. The AdV showed a high level of expression of the target gene under the control of a tissue/cancer-specific promoter, maintaining a very strict specificity. We observed that (i) because the vector was a first-generation AdV, it could be prepared on a large-scale without difficulty, and (ii) although a leak in Cre expression was observed during its preparation in *E. coli* and 293 cells, both problems were solved using a dominant-negative of Cre, dnCreRY, and an shRNA against Cre, shCreD, respectively. The complete suppression of Cre expression in 293 cells has been especially problematic, since AdV genome replication produces up to ~100 000 genome copies in each 293 cell. The key step in the production of the double-unit AdV was the selection of a clone lacking the AxL-AC virus (Figure 5b, lower left). Our results showed that severe AxL-AC generation caused by the leaky expression of Cre occurred 'before' the selection of a clone lacking the AxL-AC virus and that once such a clone was obtained, problematic deletion caused by 'leaked' Cre was not observed during the second to fourth production steps. Therefore, for the production of double-unit AdV even using 293shCreD13 cells, popular AdV-production protocols producing a pool of AdVs after transfection cannot be used.

As stated in the 'Introduction' section, this vector system is obviously superior to the 'double-infection' method (3); in the latter system, two viruses must be simultaneously transduced into a single cell for expression, and the infection of only one virus in a single cell is useless but causes similar viral toxic effects. Therefore, this new system will be particularly useful under diluted conditions, such as in animal experiments for basic research (unpublished data) as well as human gene therapy. Here, AFP promoter was used as one example, but obviously any tissue/cancer-specific promoter can be used. We intentionally did not adopt a CMV or CAG promoter, but instead used an EF1α promoter as a potent and non-specific promoter in the target unit because we have previously shown that the EF1α promoter hardly induces any inflammation as a result of AdV infection in an *in vivo* experiment, since no detectable induction of viral pIX production occurs (29). One report describing 'excisional expression' where a gene product was expressed only after excision by Cre from a Cre-excised circular molecule as described here has been previously published (30), but the purpose of this previous report was entirely different from that of the present work because the objective of the previous study was to examine persistent expression as a circular replicon using EB-viral oriP and used a double infection system using Cre-expressing AdV. Also, Yant *et al.* (31) reported another type of the 'excisional expression', where intron-containing transgenes were split and thus remained inactive until an FLP-mediated circularization restored the correct reading frame. The excision of an expression unit from the AdV genome by Cre or FLP has occasionally been reported (for examples, 32–34).

We observed a 'leak' in the expression level of the double-unit vector in an AFP-negative cell population amounting to ~1/40th of the expression level in HuH-7 cells measured using FACS as the total sum of all cell florescence, as stated in the Results section. While this level was very low, it was similar to the activity of the authentic AFP promoter in HuH-7 cells (Table 3). However, in AFP-negative cells infected with a double-unit virus, a small number of 'bright cells' highly expressing dsRed (Figure 6b, e and c, f) were present, increasing the apparent 'leaked' expression level.

Importantly, the specificity of the tissue/cancer promoter in this vector was very strictly maintained for a number of reasons. (i) Because the potent EF1α promoter in the target unit is present 'downstream' of the cDNA (Figure 1), an expression leak of the cDNA via this promoter is not possible until the promoter is translocated in front of the target cDNA by *lox*P recombination and circularization. (ii) The *lox*P-combined virus AxL-AC generated during the preparation of the double-unit virus does not contain an expression unit and hence does not cause non-specific expression. In contrast, the double-infection method always generates some stuffer-less, *lox*P-combined virus that causes non-specific expression because a small amount of such virus is generated even without Cre gene in AdV preparations, possibly through the homologous recombination of ~50 nt consisting of *lox*Ps and its surrounding sequences (3). (iii) Though conventional viral stock contains a small amount of circular DNA expressing the target gene and causing non-specific expression, it can be completely removed using a CsCl step gradient (22), since the DNA is much heavier than the virus particle. We previously observed that a DNA molecule in the viral stock can be 'transfected' into infected cells (35). (iv) The tissue-/cancer-specific promoter is inserted at the E4 position and is located farthest from the enhancer of a potent and non-specific EF1α promoter inserted at the E1-insertion site present near the left end of the genome. Therefore, the enhancer effect of the EF1α promoter on the specific AFP promoter is minimized. (v) A poly(A) sequence in front of the specific AFP promoter in the switch unit (Figure 1, upper right) suppresses non-specific transcription through a cryptic promoter present upstream of the specific promoter (3). And finally (vi) another poly(A) sequence in front of the *lox*P-cDNA in the target unit (Figure 1, upper left, and Figure 3) efficiently reduce the non-specific expression of cDNA probably caused by upstream cryptic promoters. We cannot argue whether the double-unit system is better in selectivity and less 'leaky' than the

authentic AFP promoter used here; for such conclusion further studies are needed using a more sensitive reporter system. However, because of these reasons above, the double-unit vector copes with high-level expression and strict specificity.

The total length of the AdV genome used in this method should not be more than ~38 kb (28). This means that the maximum length of a specific promoter plus target cDNA in this vector system with *Bsu*36I-*Blp*I E3 deletion (see below) should be 3.9 kb when the 14EF1α promoter is used and 4.5 kb when the 0.8-kb CMV promoter is used. This limitation of the length does not cause a problem in most cases. For example, because the AFP promoter used here is 2.2 kb in length, herpes thymidine-kinase cDNA (1.2 kb) or luciferase cDNA (1.7 kb) can be inserted; in fact, we constructed a double-unit AdV containing both AFP promoter and the thymidine-kinase gene, and animal experiments examining suicide-gene therapy are presently underway.

The problem of the genome length limitation can be solved using an AdV with a larger deletion in the E3 and E4 region. In the present study, AxLR14EL-AC and AxLR16EL-AC carried a *Bsu*36I-*Blp*I E3 deletion of 2433 bp, corresponding to 28 342–30 775-nt positions in the adenovirus type 5 map. The E3 region was 555-bp shorter than the *Xba*I-*Xba*I deleted E3 (21,27) and 252-bp longer than the *Bgl*II-*Bgl*II deleted E3 (36,37). We avoided using the *Bgl*II-*Bgl*II deleted E3 because L4 mRNAs of this AdV miss the L4 poly(A) sequences but use E3 poly(A) sequences, while *Xba*I-*Xba*I and *Bsu*36I-*Bpl*I deleted E3 both use the authentic L4 poly(A) sequences. Since an even shorter E3 region (27 865–30 995 nt) (36,38) and an E4 deletion (32 825–35 640 nt) (38) have been reported, the 3.9-kb limitation of the total lengths of a specific promoter plus cDNA when using AxLR14EL-AC could be enlarged up to 7.4 kb, if these vector constructs could be used.

Interestingly, Huyn *et al.* (39) recently reported an apparently related but different AdV system where, as the switch unit, a cancer-specific promoter produces a Gal4-VP16 fusion protein and, as the target unit, a Gal4-binding domain plus a CMV minimal promoter is used. They claimed that their method might be useful for visualizing cancer metastasis. A comparison of our vector with theirs would be difficult because they confirmed promoter specificity only in transfection experiments and because a cancer-specific promoter different from ours was used. Since our vector was developed with the goals of not only achieving a high expression level, but also of achieving a very low background in applications and ensuring the safety of gene therapy, the purposes of these studies are clearly different.

The method described here was totally different from that used for cancer-specific, replication-competent AdVs (for reviews, see references 40,41) in the field of cancer gene therapy. Although these AdVs use cancer-specific promoters, the adenoviruses replicate in the target cells and produce damaging effects through adenovirus gene expression in the target and surrounding cells. Although it has been reported that replication of E1-dereted AdV can be detected by Southern hybridization technique in HeLa cells at a higher MOI (42) and in other certain cells two weeks after infection (43), the replication level seemed too low to influence on the results described here.

The AdV system described here is probably useful for studying the function of a gene product in a specific tissue or organ. In any given tissue, several different sorts of cells are present: for example, neurons, glia cells and vascular endothelial cells are simultaneously present in neural tissue. Thus, this vector would be useful for expressing a gene selectively and efficiently in only one type of cell using a cell-specific promoter. This activity could enable novel, specific and effective therapies to be eveloped in the field of cancer gene therapy, and this strategy is now being tested. Furthermore, the application of this vector could be extended to include those where a high expression level and a rigid specificity are necessary.

The vector described here will be useful for many researchers using tissue/cancer-specific promoters. Plasmids suppressing Cre activity, cosmid cassettes for the construction of double-unit AdV containing *trc*-dnCreRY, and the 293 cell lines 293dnCreRY8 and 293shCreD13 are available from Riken Bioresource Bank (http://www.brc.riken.go.jp/) or in collaboration basis.

SUPPLEMENTARY DATA

Supplementary data are available at NAR Online.

ACKNOWLEDGMENTS

The authors thank Ms E. Kondo for her excellent secretarial assistance.

FUNDING

This work was supported by the Grant in Aid for Scientific Research on Priority Areas from Ministry of Education, Culture, Sports, Science and Technology, Japan (to I.S.). Funding for open access charge: Institute of Medical Science, University of Tokyo.

Conflict of interest statement. None declared.

REFFERENCES

1. Niwa,H., Yamamura,K. and Miyazaki,J. (1991) Efficient selection for high-expression transfectants with a novel eukaryotic vector. *Gene*, **108**, 193–199.
2. Kim,D.W., Uetsuki,T., Kaziro,Y., Yamaguchi,N. and Sugano,S. (1990) Use of the human elongation factor 1 alpha promoter as a versatile and efficient expression system. *Gene*, **91**, 217–223.
3. Sato,Y., Tanaka,K., Lee,G., Kanegae,Y., Sakai,Y., Kaneko,S., Nakabayashi,H., Tamaoki,T. and Saito,I. (1998) Enhanced and specific gene expression via tissue-specific production of Cre recombinase using adenovirus vector. *Biochem. Biophys. Res. Commun.*, **244**, 455–462.
4. Wilson,C., Bellen,H.J. and Gehring,W.J. (1990) Position effects on eukaryotic gene expression. *Annu. Rev. Cell Biol.*, **6**, 679–714.

5. Giraldo,P. and Montoliu,L. (2001) Size matters: use of YACs, BACs and PACs in transgenic animals. *Transgenic Res.*, **10**, 83–103.
6. Kijima,T., Osaki,T., Nishino,K., Kumagai,T., Funakoshi,T., Goto,H., Tachibana,I., Tanio,Y. and Kishimoto,T. (1999) Application of the Cre recombinase/*lox*P system further enhances antitumor effects in cell type-specific gene therapy against carcinoembryonic antigen-producing cancer. *Cancer Res.*, **59**, 4906–4911.
7. Ueda,K., Iwahashi,M., Nakamori,M., Nakamura,M., Yamaue,H. and Tanimura,H. (2000) Enhanced selective gene expression by adenovirus vector using Cre/*lox*P regulation system for human carcinoembryonic antigen-producing carcinoma. *Oncology*, **59**, 255–265.
8. Ueda,K., Iwahashi,M., Nakamori,M., Nakamura,M., Matsuura,I., Yamaue,H. and Tanimura,H. (2001) Carcinoembryonic antigen-specific suicide gene therapy of cytosine deaminase/5-fluorocytosine enhanced by the cre/*lox*P system in the orthotopic gastric carcinoma model. *Cancer Res.*, **61**, 6158–6162.
9. Goto,H., Osaki,T., Kijima,T., Nishino,K., Kumagai,T., Funakoshi,T., Kimura,H., Takeda,Y., Yoneda,T., Tachibana,I. *et al.* (2001) Gene therapy utilizing the Cre/*lox*P system selectively suppresses tumor growth of disseminated carcinoembryonic antigen-producing cancer cells. *Int. J. Cancer*, **94**, 414–419.
10. Ueda,K., Iwahashi,M., Nakamori,M., Nakamura,M., Matsuura,I., Ojima,T. and Yamaue,H. (2003) Improvement of carcinoembryonic antigen-specific prodrug gene therapy for experimental colon cancer. *Surgery*, **133**, 309–317.
11. Nagayama,Y., Nishihara,E., Iitaka,M., Namba,H., Yamashita,S. and Niwa,M. (1999) Enhanced efficacy of transcriptionally targeted suicide gene/prodrug therapy for thyroid carcinoma with the Cre-*lox*P system. *Cancer Res.*, **59**, 3049–3052.
12. Sakai,Y., Kaneko,S., Sato,Y., Kanegae,Y., Tamaoki,T., Saito,I. and Kobayashi,K. (2001) Gene therapy for hepatocellular carcinoma using two recombinant adenovirus vectors with alpha-fetoprotein promoter and Cre/*lox* P system. *J. Virol. Methods*, **92**, 5–17.
13. Yoshimura,I., Ikegami,S., Suzuki,S., Tadakuma,T. and Hayakawa,M. (2002) Adenovirus mediated prostate specific enzyme prodrug gene therapy using prostate specific antigen promoter enhanced by the Cre-*lox*P system. *J. Urol.*, **168**, 2659–2664.
14. Maeda,M., Namikawa,K., Kobayashi,I., Ohba,N., Takahara,Y., Kadono,C., Tanaka,A. and Kiyama,H. (2006) Targeted gene therapy toward astrocytoma using a Cre/*lox*P-based adenovirus system. *Brain Res.*, **1081**, 34–43.
15. Namikawa,K., Murakami,K., Okamoto,T., Okado,H. and Kiyama,H. (2006) Efficient generation of recombinant adenoviruses using adenovirus DNA-terminal protein complex and a cosmid bearing the full-length virus genome. *Gene Ther.*, **13**, 1244–1250.
16. Graham,F.L., Smiley,J., Russell,W.C. and Nairn,R. (1977) Characteristics of a human cell line transformed by DNA from human adenovirus type 5. *J. Gen. Virol.*, **36**, 59–74.
17. Aden,D.P., Fogel,A., Plotkin,S., Damjanov,I. and Knowles,B.B. (1979) Controlled synthesis of HBsAg in a differentiated human liver carcinoma-derived cell line. *Nature*, **282**, 615–616.
18. Nakabayashi,H., Taketa,K., Miyano,K., Yamane,T. and Sato,J. (1982) Growth of human hepatoma cells lines with differentiated functions in chemically defined medium. *Cancer Res.*, **42**, 3858–3863.
19. Fogh,J., Fogh,J.M. and Orfeo,T. (1977) One hundred and twenty-seven cultured human tumor cell lines producing tumors in nude mice. *J. Natl Cancer Inst.*, **59**, 221–226.
20. Ido,A., Nakata,K., Kato,Y., Nakao,K., Murata,K., Fujita,M., Ishii,N., Tamaoki,T., Shiku,H. and Nagataki,S. (1995) Gene therapy for hepatoma cells using a retrovirus vector carrying herpes simplex virus thymidine kinase gene under the control of human alpha-fetoprotein gene promoter. *Cancer Res.*, **55**, 3105–3109.
21. Fukuda,H., Terashima,M., Koshikawa,M., Kanegae,Y. and Saito,I. (2006) Possible mechanism of adenovirus generation from a cloned viral genome tagged with nucleotides at its ends. *Microbiol. Immunol.*, **50**, 643–654.
22. Kanegae,Y., Makimura,M. and Saito,I. (1994) A simple and efficient method for purification of infectious recombinant adenovirus. *Jpn. J. Med. Sci. Biol.*, **47**, 157–166.
23. Sambrook,J. and Russell. (1989) *Molecular Cloning: A Laboratory Manual*, Vol. 1, 3rd edn. Cold Spring Harbor Laboratory Press, Cold Spring Harbor, NY.
24. Kanegae,Y., Takamori,K., Sato,Y., Lee,G., Nakai,M. and Saito,I. (1996) Efficient gene activation system on mammalian cell chromosomes using recombinant adenovirus producing Cre recombinase. *Gene*, **181**, 207–212.
25. Saito,I., Oya,Y., Yamamoto,K., Yuasa,T. and Shimojo,H. (1985) Construction of nondefective adenovirus type 5 bearing a 2.8-kilobase hepatitis B virus DNA near the right end of its genome. *J. Virol.*, **54**, 711–719.
26. Kondo,S., Takata,Y., Nakano,M., Saito,I. and Kanegae,Y. (2009) Activities of various FLP recombinases expressed by adenovirus in mammalian cells. *J. Molec. Biol.*, **390**, 221–230.
27. Miyake,S., Makimura,M., Kanegae,Y., Harada,S., Sato,Y., Takamori,K., Tokuda,C. and Saito,I. (1996) Efficient generation of recombinant adenoviruses using adenovirus DNA-terminal protein complex and a cosmid bearing the full-length virus genome. *Proc. Natl Acad. Sci. USA*, **93**, 1320–1324.
28. Bett,A.J., Prevec,L. and Graham,F.L. (1993) Packaging capacity and stability of human adenovirus type 5 vectors. *J. Virol.*, **67**, 5911–5921.
29. Nakai,M., Komiya,K., Murata,M., Kimura,T., Kanaoka,M., Kanegae,Y. and Saito,I. (2007) Expression of pIX gene induced by transgene promoter: possible cause of host immune response in first-generation adenoviral vectors. *Hum. Gene Ther.*, **18**, 925–936.
30. Leblois,H., Roche,C., Di Falco,N., Orsini,C., Yeh,P. and Perricaudet,M. (2000) Stable transduction of actively dividing cells via a novel adenoviral/episomal vector. *Mol. Ther.*, **1**, 314–322.
31. Yant,S.R., Ehrhardt,A., Mikkelsen,J.G., Meuse,L., Pham,T. and Kay,M.A. (2002) Transposition from a gutless adeno-transposon vector stabilizes transgene expression in vivo. *Nat. Biotechnol.*, **20**, 999–1005.
32. Gil,J.S., Gallaher,S.D. and Berk,A.J. (2010) Delivery of an EBV episome by a self-circularizing helper-dependent adenovirus: long-term transgene expression in immunocompetent mice. *Gene Ther.*, doi:10.1038/gt.2010.75.
33. Dorigo,O., Gil,J.S., Gallaher,S.D., Tan,B.T., Castro,M.G., Lowenstein,P.R., Calos,M.P. and Berk,A.J. (2004) Development of a novel helper-dependent adenovirus-Epstein-Barr virus hybrid system for the stable transformation of mammalian cells. *J. Virol.*, **78**, 6556–6566.
34. Lee,J.H., Yi,S.M., Anderson,M.E., Berger,K.L., Welsh,M.J., Klingelhutz,A.J. and Ozbun,M.A. (2004) Propagation of infectious human papillomavirus type 16 by using an adenovirus and Cre/*Lox*P mechanism. *Proc. Natl Acad. Sci. USA*, **101**, 2094–2099.
35. Nakano,M., Odaka,K., Takahashi,Y., Ishimura,M., Saito,I. and Kanegae,Y. (2005) Production of viral vectors using recombinase-mediated cassette exchange. *Nucleic Acids Res.*, **33**, e76.
36. Bett,A.J., Haddara,W., Prevec,L. and Graham,F.L. (1994) An efficient and flexible system for construction of adenovirus vectors with insertions or deletions in early regions 1 and 3. *Proc. Natl Acad. Sci. USA*, **91**, 8802–8806.
37. Mizuguchi,H. and Kay,M.A. (1998) Efficient construction of a recombinant adenovirus vector by an improved in vitro ligation method. *Hum. Gene Ther.*, **9**, 2577–2583.
38. Mizuguchi,H. and Kay,M.A. (1999) A simple method for constructing E1- and E1/E4-deleted recombinant adenoviral vectors. *Hum. Gene Ther.*, **10**, 2013–2017.
39. Huyn,S.T., Burton,J.B., Sato,M., Carey,M., Gambhir,S.S. and Wu,L. (2009) A potent, imaging adenoviral vector driven by the cancer-selective mucin-1 promoter that targets breast cancer metastasis. *Clin. Cancer Res.*, **15**, 3126–3134.

40. Toth,K., Dhar,D. and Wold,W.S. (2010) Oncolytic (replication-competent) adenoviruses as anticancer agents. *Expert Opin. Biol. Ther.*, **10**, 353–368.
41. Mathis,J.M., Stoff-Khalili,M.A. and Curiel,D.T. (2005) Oncolytic adenoviruses – selective retargeting to tumor cells. *Oncogene*, **24**, 7775–7791.
42. Steinwaerder,D.S., Carlson,C.A. and Lieber,A. (2001) Human papilloma virus E6 and E7 proteins support DNA replication of adenoviruses deleted for the E1A and E1B genes. *Mol. Ther.*, **4**, 211–216.
43. Ghosh,S. and Duigou,G.J. (2005) Decreased replication ability of D1-deleted adenoviruses correlates with increased brain tumor malignancy. *Cancer Res.*, **65**, 8936–8943.

 AJRCMB Articles in Press. Published on December 3, 2010 as doi:10.1165/rcmb.2010-0092OC

Keratinocyte growth factor gene transduction ameliorates pulmonary fibrosis induced by bleomycin in mice

Seiko Sakamoto[1], Takuya Yazawa[2], Yasuko Baba[1], Hanako Sato[2], Yumi Kanegae[3], Toyohiro Hirai[4], Izumu Saito[3], Takahisa Goto[1], Kiyoyasu Kurahashi[1]

[1]Department of Anesthesiology and Critical Care Medicine and [2]Department of Pathology, Yokohama City University Graduate School of Medicine, Yokohama 236-0004, Japan.

[3]Laboratory of Molecular Genetics, Institute of Medical Science, University of Tokyo, Tokyo 108-0071, Japan.

[4]Department of Respiratory Medicine, Graduate School of Medicine, Kyoto University, Kyoto 606-8507, Japan

Address for reprint requests and other correspondence: K. Kurahashi, Dept. of Anesthesiology and Critical Care Medicine, Yokohama City Univ. Graduate School of Medicine, 3-9 Fukuura, Kanazawa-ku, Yokohama 236-0004, Japan (e-mail: kiyok@med.yokohama-cu.ac.jp).

Running title:

KGF gene ameliorates pulmonary fibrosis

Grant and funding:

This study was supported in part by Japan Society for the Promotion of Science Grants-in-Aid for Scientific Research nos. 18591987 and 20390459 (to K. Kurahashi) and the Yokohama Foundation for the Advancement of Medical Science, Umehara Fund (to K. Kurahashi).

This article has an online data supplement, which is accessible from this issue's table of content online at www.atsjournals.org

Abstract

Pulmonary fibrosis has high rates of mortality and morbidity, but there is no established therapy at present. We demonstrate here that bleomycin-induced pulmonary fibrosis in mice is ameliorated by intratracheal administration of keratinocyte growth factor (KGF)-expressing adenovirus vector (Ad-KGF). Progressive pulmonary fibrosis was created by continuous subcutaneous administration of 120 mg/kg of bleomycin subcutaneously using an osmotic pump twice from Day 1 to 7 and Day 29 to 35. The mice initially exhibited subpleural fibrosis, and then advanced fibrosis in the parenchyma of the lungs. These histopathological changes were accompanied by reduced lung compliance (0.041 ± 0.011 vs. 0.097 ± 0.004; $p < 0.001$), reduced messenger expression of surfactant proteins, and reduced KGF messenger expression in the lungs at 4 weeks compared with naïve group. Intratracheal instillation of Ad-KGF at 1 week after the first administration of bleomycin increased KGF mRNA expression in the lungs compared with the fibrosis-induced mice that received saline alone. The phenotype was associated with alveolar epithelial cell proliferation, increased pulmonary compliance (0.062 ± 0.005 vs. 0.041 ± 0.011; $p = 0.023$), and decreased mortality (survival rate on Day 56: 68.8% vs. 0%; $p = 0.002$), compared with those received only the saline vehicle. These observations suggest the therapeutic utility of a KGF-expressing adenoviral vector for pulmonary fibrosis.

Keywords:

keratinocyte growth factor, pulmonary fibrosis, gene therapy, adenovirus

Introduction

Pulmonary fibrosis is refractory to treatment regardless of its etiology. International consensus statements conclude that existing therapies for idiopathic pulmonary fibrosis (IPF) are of unproven benefit and emphasize the need to develop novel therapies (1). Development of pulmonary fibrosis depends heavily on alveolar epithelial injury and aberrant repair (2). Persistent inflammation, tissue necrosis, and infection lead to chronic myofibroblast activation and excessive accumulation of extra-cellular matrix components, which promote the formation of a permanent fibrotic scar (3). Modulation of the alveolar repair process is a potential therapeutic target.

Bleomycin, an antitumor antibiotic, binds to DNA and inhibits DNA-dependent RNA synthesis (4). One of the major side effects of this drug is pulmonary fibrosis (5). The pathogenesis of this side effect has been examined in animals (6, 7), and bleomycin has been used to create fibrosis in animal experimental models to elucidate a therapy for pulmonary fibrosis in patients.

Keratinocyte growth factor (KGF) is a potent mitogenic factor for alveolar epithelial cells whose specific receptor is expressed on epithelial cells (8). KGF has many properties that may be beneficial in treating pulmonary fibrosis. For example, KGF stimulates type II pneumocyte proliferation (9), increases surfactant protein production (10), increases alveolar epithelial fluid transportation (11), decreases apoptosis (12-16), and promotes DNA repair (17). However, KGF protein has so far demonstrated only limited effectiveness in various models of acute lung injury including hyperoxia-, radiation-, and bleomycin-induced lung injury (18-21). This is perhaps because KGF protein has a short duration of action. To overcome this issue, we previously used a KGF-expressing adenovirus vector (Ad-KGF) in a mouse model of hyperoxia-induced lung injury (22). In our previous study, we demonstrated that intratracheal administration of Ad-KGF resulted in over-expression of KGF for 7 days, attenuated lung injury, and decreased mortality when the animals were observed for up to 11 days after KGF transduction. In all the previous studies including ours, KGF was administered preventatively, *i.e.*, *before* the lung injury was created. It is yet unknown whether KGF is beneficial when administered *after* the insults to the lung have been incurred.

The purpose of this study was to elucidate whether Ad-KGF ameliorated bleomycin-induced pulmonary fibrosis when it was administered 7 days after bleomycin was started.

Materials and methods

Generation of recombinant adenovirus

We used a recombinant adenovirus (rAd) expressing murine KGF cDNA under the control of a potent CAG promoter (23) (AxCAmKGF denoted Ad-KGF in this paper), which was previously reported (22) (**Fig. 1-i**). Ax1w1, which bears no insert, including any promoter, cDNA, or poly(A) sequence (24), denoted Ad-1w1 in this paper was used as a control (**Fig. 1-ii**).

Experimental protocol